Evaluating the Utility of Short-term Hydrological Forecasts in a Hydropower System

Mémoire

Hajar Nikghalb Ashouri

Maîtrise en génie civil – Génie des eaux
Maître ès sciences (M. Sc.)

Québec, Canada

Evaluating the Utility of Short-term Hydrological Forecasts in a Hydropower System

Mémoire

Hajar Nikghalb Ashouri

Sous la direction de:

Amaury, Tilmant directeur de recherche

Résumé

Le fonctionnement optimal d'un système de réservoirs est un processus décisionnel complexe impliquant, entre autres, l'identification d'un compromis temporel concernant l'utilisation de l'eau : la dernière unité d'eau doit-elle être conservée ou plutôt utilisée pour un usage immédiat ? La variabilité des apports hydrologiques complique encore davantage ce processus décisionnel puisque la recherche de ce compromis doit être effectuée sans une connaissance parfaite des conditions futures. De manière générale, l'équilibre optimal entre les utilisations immédiates et futures de l'eau nécessite l'intégration de règles de gestion à court et à long terme. Si les règles à court terme conduisent à des décisions à courte vue, les stratégies opérationnelles à long terme ne sont pas appropriées pour gérer des événements à court terme tels que les inondations. Nous proposons un cadre de modélisation basé sur l'approche de décomposition temporelle (DT) : Les stratégies à moyen/long terme sont tout d'abord déterminées puis utilisées comme limites pour l'optimisation des stratégies à court terme. Le modèle d'optimisation à moyen terme capture la persistance temporelle trouvée dans le processus des apports hydrologiques hebdomadaires, alors que les prévisions hydrologiques d 'ensemble (PHE) sont utilisées pour piloter le modèle à court terme sur un pas de temps journalier. Plus spécifiquement, la programmation dynamique stochastique duale (SDDP) génère les fonctions des bénéfices de valeur hebdomadaires qui sont ensuite imposées à un modèle de programmation linéaire implémenté sur chaque membre des PHE de 14 jours. Ce cadre de modélisation est mis en œuvre selon un mode de gestion en horizon roulant sur une cascade de centrales hydroélectriques dans le bassin de la rivière Gatineau dans la province du Québec au Canada. À l'aide de ce cadre de modélisation, nous analysons la relation entre la valeur économique et les caractéristiques statistiques des PHE. Les résultats montrent que l'énergie générée par le système hydroélectrique augmente avec la précision et la résolution de la prévision, mais que la relation n'est pas univoque. En effet, d'autres facteurs semblent contribuer à l'utilité de la prévision.

Abstract

The optimal operation of a system of reservoirs is a complex decision-making problem involving, among others, the identification of a temporal trade-offs regarding the use of water. Should the last unit of water be kept in storage or rather be released for use downstream? The variability of natural inflows further complicates this decision-making problem: at any given point in space and time, this trade-off must be made without a perfect knowledge of future reservoir inflows. Generally speaking, the optimal balance between immediate and future uses of water requires the integration of short- and long-term policies. If short-term policies lead to shortsighted decisions, long-term operational strategies are not appropriate to handle short-term events such as floods. We propose a modeling framework based on the time decomposition (TD) approach: mid/long-term policies are determined first and then used as boundary conditions for the optimization of short-term policies. The mid-term optimization model captures the temporal persistence found in the weekly streamflow process whereas Ensemble Streamflow Forecasts (ESF) are used to drive the short-term model on a daily time step. More specifically, a Stochastic Dual Dynamic Programming (SDDP) generates the weekly benefit-to-go functions that are then imposed to a linear programming model implemented on each 14-days member of the ESF. This modelling framework is implemented in a rolling-horizon mode on a cascade of hydropower stations in the Gatineau River basin, Quebec, Canada. Using this modelling framework, we analyze the relationship between the economic value of different sets of short-term hydrologic forecasts. The results show that the energy generated by the hydropower system increases with the forecast's accuracy and resolution but that the relationship is not univocal; other factors seem to contribute to the forecast's utility.

Table des matières

Liste des tableaux

Liste des figures

Acknowledgement

I would first like to thank my thesis advisor Amaury Tilmant for guiding and supporting me to do this research. He consistently allowed this research to be my own work, but steered me in the right direction. I also appreciate his time and his patience for helping me to write this thesis.

I would also like to thank Prof. François Anctil for his valuable discussions. He was leading his team to provide the hydrological input for this research. Special thanks to Emixi Valdez in Prof. Anctil's team, who was directly providing and delivering the hydrological information for this research. I would like to thank Dr. Jasson Pina for sharing his knowledge and giving technical advice.

My Sincere thanks goes to Raheleh Amini and Ahmad Amini for their supports. I am thankful to Eric Pomerleau for his supports and continuous motivation. Special thanks to my friend, Shirin Panahi for helping me to improve my English writing. I would like to thank my family: my parents and to my brothers for supporting me spiritually.

Introduction

The reservoir operation problem is a complex multi-stage decision making problem. A sequence of release decisions must be determined so that benefits/costs are maximized/minimized taking into account various physical, operational, and legal constraints such as municipal/ industrial water supplies, minimum streamflow requirements for environmental and ecological concerns, legal agreements, contracts, etc.

Depending on whether the management problem has short- or long-term consequences, typical time-steps (stages) can be hourly, daily, weekly or monthly. At the beginning of each stage, reservoir operators face a trade-off between the immediate and future consequences of a release decision ; should the water be released or kept in the storage for future uses ? In other words, the operators face a temporal trade-off. They may also have to decide about allocating water to conflicting users which gives rise to spatial trade-off. Another complicating factor is the hydrologic uncertainty and the difficulty to accurately forecast future inflows'.

Solving the reservoir operation problem therefore requires the assistance of optimization techniques. Over the past decades, many optimization models have been proposed in the literature but no single solution has emerged. Each technique has its own strengths and weaknesses and the choice will ultimately depend on the characteristics of the system, the availability of data, the objective function and constraints as well as the operators' preference. State-of-the-art reviews about the optimization techniques for reservoir operation problem can be found in Yeh and Becker (1982), Labadie (2004), Rani and Moreira (2010) and more recently in Ahmad and El-shafie (2014).

Dynamic Programming (DP) (Bellman (1957)) is one of the most popular techniques to solve the reservoir operation problem. DP solves the optimization problem by decomposing a multistage problem into a series of single-stage problems that are solved recursively. DP performs an optimization by discretizing the continuous state variables and replacing the continuous state-space by a grid. These optimal solutions are generalized for other points of the state variables by a continuous function, using an interpolation approach (e.g. linear, cubic spline) (Tejada-Guibert et al. (1993)).

Figure 0.1 illustrates the basic principle behind the one-stage optimization problem : at each

stage, the sum of the immediate and future benefits from system operation must be maximized. Because the immediate and future uses of water are orthogonal, when the future benefits increase, immediate benefits must decrease and vice-versa. Of interest is the fact that the derivatives of the immediate and benefit-to-go functions give the immediate and future water values, respectively, which must be identical at the optimal solution (Tilmant et al. (2008)). The marginal value of water is the willingness to pay for an additional unit of water in a particular reservoir and at a given time of the year. This approach is limited to small-scale problems because computational effort increases exponentially with the number of reservoirs in the system

DP can easily be extended to solve stochastic multi-stage decision-making problems. For the reservoir operation problem, the basic idea is to include an additional, hydrologic, state variable to capture the spatial and temporal persistences found in the streamflow processes. Stochastic DP (SDP), often referred to a Markov decision process, solves the problem by discretizing stochastic variables, as well as the system status, to obtain an optimal policy for each discrete value of the reservoir system (Figure 0.2). The optimal solutions are then interpolated to the rest of the domain. Since SDP solves the problem on all discrete combinations of the state variables, its application is limited by the so-called curse of dimensionality, limited to small scale systems involving no more than four state variables (storage and hydrologic).

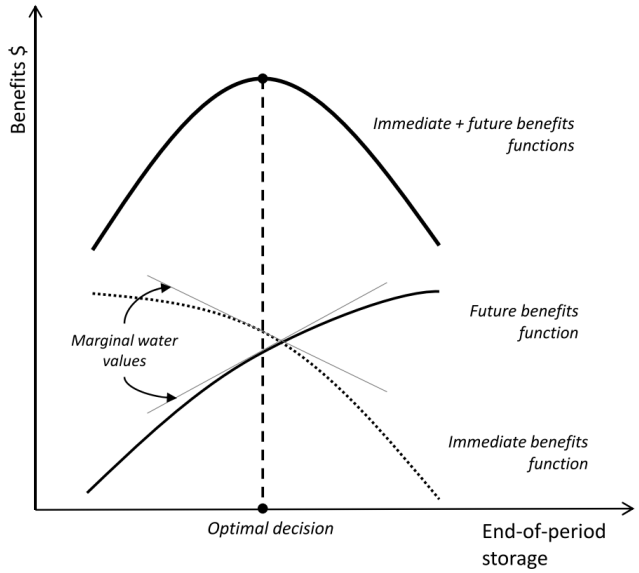

Figure 0.1 – Immediate and future benefits functions (Tilmant et al. (2008))

To address the limitations posed by the curse of dimensionality, Pereira and Pinto (1991) developed Stochastic Dual Dynamic Programming (SDDP). SDDP removes the computational burden of SDP by constructing a locally-accurate approximation of the benefit-to-go function using piecewise linear segments, which are constructed from the primal and dual solutions of the one-stage optimization problem. SDDP has been largely used in hydropower dominated

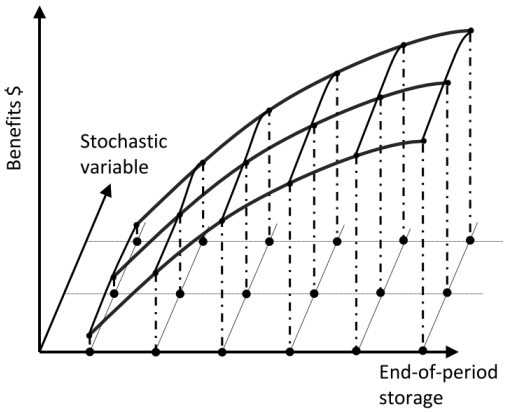

Figure 0.2 – SDP principle when maximizing the sum of immediate and future benefits functions, discretizing, and interpolating of the state variables and system status (Pina (2017))

systems in Norway (Gjelsvik et al. (2010)) , South and Central America (Pereira (1989) ; Shapiro et al. (2013)), New Zealand (Kristiansen (2004)), Euphrates-Tigris River basin (Tilmant et al. (2008)), the Nile River basin (Goor et al. (2012)), the Zambezi River basin (Tilmant and Kinzelbach (2012)), and Spain (Pereira-Cardenal et al. (2016) ; Macian-Sorribes et al. (2017)).

Moreover, to capture the hydrologic uncertainty while avoiding the discretization of the hydrologic state variable, SDDP uses a multi-site periodic auto-regressive MPAR-(p) model. Recently, various authors have proposed improvements to the built-in hydrological model for SDDP (see for example Poorsepahy-Samian et al. (2016), Raso et al. (2017), Pina et al. (2017a)).

To handle the stochastic hydrology of the hydropower system, stochastic linear programming (SLP) and Chance constrained LP (CCLP) have been proposed. SLP assumes the streamflow follow a single Markov chain. Instead of providing the steady state releases as a function of storages, SLP produces steady state probabilities of releases and storages (Loucks et al. 1981). An application of CCLP can be found in the study by Sreenivasan and Vedula (1996) to maximize hydroelectricity production of a multipurpose reservoir. Lee et al. (2006) and Seif and Hipel (2001) applied a two stage SLP approach to handle stochastic inflows.

Over the past few years, the hydrometeorological community has been progressively shifting from deterministic simulations to probabilistic ones based on ensembles. Ensemble forecasts present an alternative to traditional deterministic forecasts by providing a probabilistic assessment of future discharges. An ensemble is a collection of deterministic predictions of the same event and attempts to produce a representative sample of the future (Figure 0.3).

Ensemble Streamflow Forecasts (ESFs) can capture the following sources of uncertainty : weather forecasts, hydrological model structure and initial hydrologic conditions (Bourdin et al. (2012)). ESFs are usually produced by forcing hydrological models with meteorological forecasts, which in turn include multiple possible future trajectories of atmospheric variables

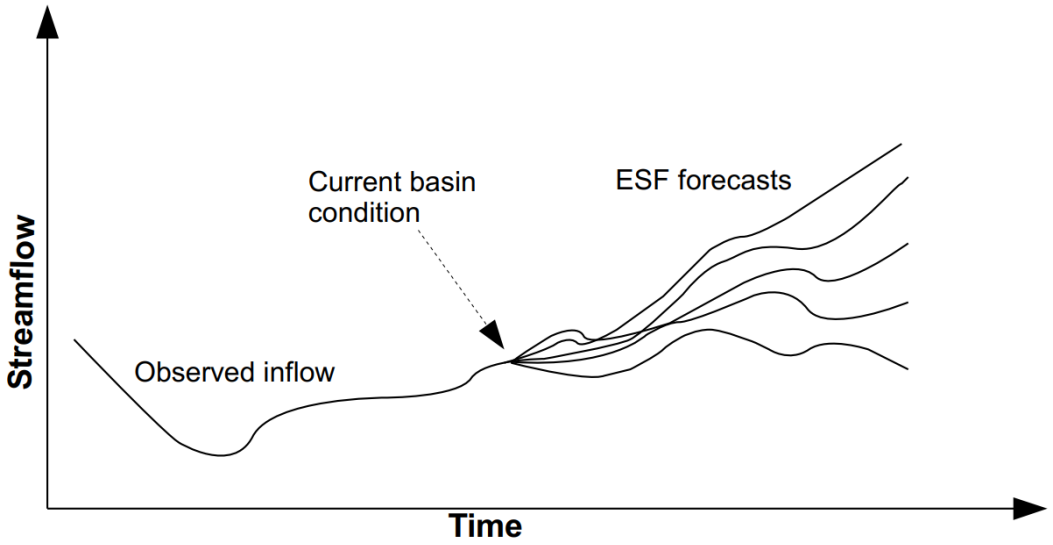

Figure 0.3 – Ensemble Streamflow Forecast (ESF) trajectories

(Cloke and Pappenberger (2009)). The initial condition uncertainty of ESFs stems from the propagation of small errors in the initial conditions of the atmospheric models (Buizza, 2003). Usually, a set of typically ten to fifty initial conditions is obtained and is used to initiate simulations. Finally, the structural uncertainty of the ESFs can be captured by pooling several hydrologic models with fundamentally different structures.

Many studies worldwide have illustrated the use of ESFs for reservoir operation. In the study of Zhao et al. (2011), synthetic experiments of ESF were applied to real-time reservoir operation and were compared with deterministic forecasts. Results showed that the benefit from using ensembles was nearly as high as the one obtained with a perfect forecast. Boucher et al. (2012) determined the economic benefits associated with ESFs for a flood event on the Gatineau River, Canada. Ficchì et al. (2015) assessed the improvement of a four-reservoir system in the Seine River basin, France, using an ensemble of weather forecasts and a real-time control approach. Fan et al. (2016) examined the added value of applying ESFs comapred to deterministic forecasts for short-term reservoir operation of a hydropower system in Brazil.

For many reservoir operation problems, the forecast horizon (FH) is usually shorter than the reservoir operation horizon (OH). FH represents the length of time in the future that inflow predictions are generated. This generally may vary from one hour, day, week, or month ; however, OH represents the length of time that the reservoir operation is targeted which can vary from several months to several years. For example, the operation of a reservoir for flood control purposes may extend over several months while a streamflow forecast is only available a few weeks in advance. To bridge the gap between OH and FH, the Rolling Horizon (RH) technique can be implemented. It consists in dynamically simulating the system, adjusting release decisions on a daily time step based on the storage level at the beginning of the day

and updated hydrologic forecasts. (It consists in dynamically simulating the system, adjusting release decisions on decision horizon (DH) based on the storage level at the beginning of the DH and updated hydrologic forecasts. The decision horizon (DH) represents how long the generated decision is implemented. As inflow forecasts update day by day, DH is usually set as one day. This suggests that only the current period decision is regarded as final and decisions in the future periods will be updated with a new forecast.)

You and Cai (2008) applied rolling horizon concept to determine the optimal forecast horizon (FH) based on a given decision horizon (DH) for dynamic reservoir operation problems. They identified the impact of various factors such as water stress level (the deficit between water availability and demand), reservoir size, inflow uncertainty, evaporation rate, and discount rate. Their results show that inflow characteristics and reservoir capacity have major impacts on FH when water stress is modest ; larger reservoir capacity and the deterministic component of inflow such as seasonality require a longer FH. Economic factors have strong impacts when water stress levels are high. Zhao et al. (2012) compared the impact of forecast horizon (FH) and forecast uncertainty (FU) to find the effective forecast horizon (EFH) for real-time reservoir operation in a rolling-horizon scheme. Wang et al. (2014) employed the rolling horizon approach and distributed hydrological inflow predictions to determine real-time reservoir releases, for a three-reservoir system in the Red River Basin in Southeast Asia. Arena et al. (2017) developed an optimization- simulation system based on RH for operating a real-word two-reservoir system in Italy. Séguin et al. (2017) applied a rolling horizon simulation scheme to develop a daily hydropower operations planning using a stochastic short-term optimization model based on scenario trees to represent the uncertainty of inflows.

In general, hydrologic forecasts are available for different horizons (short, mid and log-term). Although short-term forecasts are in general reliable, their limited horizon (ranging from one hour to a few days) makes them useless for water resource systems characterized by large carryover storage capacity. Long-term streamflow forecast, on the other hand, are potentially more interesting for those systems but their precision is often too low (Zhao and Zhao (2014)). In contrast, the operation of a reservoir system with limited storage capacity will benefit from regularly updated short-term forecasts (while long-term forecasts are in this case useless).

Yao and Georgakakos (2001)) proposed an approach integrating long- and short-term streamflow forecasts to operate the Folsom reservoir in California. The approach relies on time decomposition (TD) : the long-term problem is solved first and then the solutions are passed to the short-term problem where they are used as boundary conditions. Typically, target storage levels at the end of the week (month) or weekly (monthly) water values are imposed on the short-term model. Many researchers have applied TD to solve the reservoir operation problem. For example, Yeh and Becker (1982) apply the traditional nesting TD over three levels : monthly, daily, and hourly. Zahraie and Karamouz (2004) develop a TD approach in which SDP formulations handle the long-term and midterm problems, while a DP model take care of

the short-term optimization of a two-reservoirs system. Georgakakos (2006) use TD to develop a multi-layer operation model, covering real-time, mid-term, and long-term layers for the Nile basin. Alemu et al. (2011) propose a decision support system can exploit ensemble streamflow prediction (ESP). The long-term model is based on simulation, which provides guides for short-term optimization based upon historic reservoir operating policies. Zhao and Zhao (2014) applied a combination of short- and long-term forecasts to derive short- and long-term operational policies for a single reservoir in China. They used a traditional nesting TD to pass the optimized long-term storage to short-term model as a boundary condition.

Even though TD reduces the computational effort required to solve the reservoir operation problem, researchers and practitioners still face a trade-off between system and hydrologic complexity. This trade-off essentially exists because traditional optimization techniques cannot handle a large number of reservoirs (system complexity) or process a large quantity of hydrologic information (hydrologic complexity).

This study addresses the above challenge by combining, within a TD framework, relevant optimization techniques so that a mix of short and long-term forecasts can be processed over potentially large hydropower systems without undue computation time. The proposed framework is applied to Gatineau River basin, a hydropower system, located in Quebec (Canada). The system includes three reservoirs and four hydropower plants with an installed capacity of more than 500 MW. Because the Gatineau River basin consists of inhabited areas, the main operating constraints are related to the production of hydroelectricity. Unfortunately, the operator did not share the information regarding the current operation of the system. There are some considerations about boating and recreational activities, supplying the drinking water of nearby towns and flood risks in Gatineau River basin. More details are presented in Chapitre 2.

The optimal decisions based on the proposed approach will benefit from the reliability of the short-term forecast and the longer horizon of the mid-term forecasts. The weekly water values are determined via the mid-term (weekly) optimization model SDDP. They are then processed by the short-term optimization model to make sure the short-term operation respect the future demands. At the beginning of each day, the short-term model seeks to maximize the production of energy along each member over the next 14 days taking into account the value of water at the end of that period. The next day, the process is repeated using updated ESF. Since each ESF has 50 members and with a planning period extending over 6 years, the short-term reservoir operation model is formulated as a LP in order to keep the computation time within reasonable limits. The modelling framework is then used to explore the economic value of the hydrological forecasts generated by 20 different hydrologic models.

The thesis is organized as follows : section 2 starts with a presentation of temporal decomposition (TD) which is then followed by a description of the mid-term (MT) model and

integration of MT and short-term (ST) model, then the section ends with the case study following by application of the modeling framework to the Gatineau River basin. Analysis of simulation results are discussed in section 3. Finally, conclusion is given in section 4.

Chapitre 1

Materials and Methods

1.1 Time Decomposition (TD)

Time Decomposition (TD) is a conventional approach to connect the operation with different time scales (Figure 1.1, Karamouz et al. (2003), Lamontagne and Stedinger (2014)). In this study we make the distinction between short and mid-term operation. Mid-term operation determines of weekly releases over a planning horizon of several years and provides the seasonal trajectory that the system should follow in order to sustain the production of energy in a "distant" future (beyond the horizon). Short-term operation is concerned with the determination of daily releases over a period of 14 days corresponding to the horizon of the regularly-updated ESF.

As mentioned earlier, the mid-term reservoir operation problem is solved by SDDP, whose weekly benefit-to-go functions are then passed to the short-term optimization problem, which is formulated as a LP implemented on each member on a daily basis. Both models are thus connected through the SDDP-derived benefit-to-go functions, meaning that no restrictions are imposed on the decision variables (release and storage) of the lower-level, short-term, LP model. The precision of the terminal value function of the upper-level model plays an important role for the accuracy of the results of the lower-level model. For instance, if a weekly model overestimates the terminal value of storage at the end of each time step, the lower-level model will attempt to refill the reservoir in each time step and vice versa.

1.2 Problem formulation

The objective of a reservoir operation problem is to determine a sequence of optimal decisions that maximize the benefits of the system operation over a given planning horizon considering physical, operational, and institutional constraints (Figure 1.2).

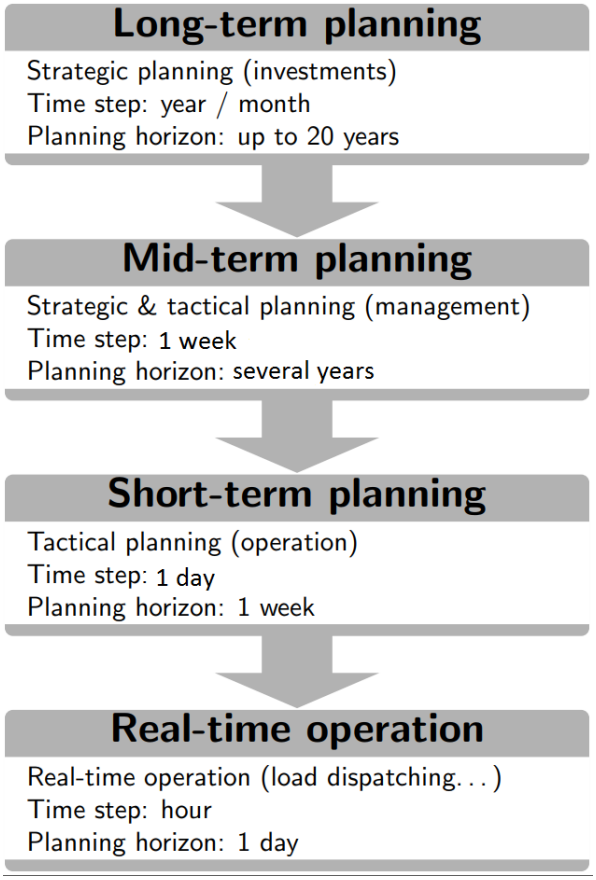

Figure 1.1 – Time decomposition for the reservoir operation problem

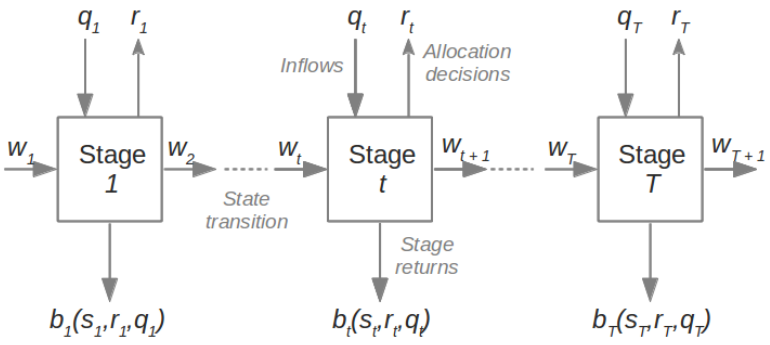

Figure 1.2 – Multi-stage decision making problem scheme (Labadie (2004))

Mathematically, the multistage decision-making problem can be written as :

$$Z = \max_{\boldsymbol{x}_t} \left\{ \mathop{\mathbb{E}}_{\boldsymbol{q}_t} \left[\sum_{t=1}^{T} \alpha_t b_t(\boldsymbol{s}_t, \boldsymbol{x}_t, \boldsymbol{q}_t) + \alpha_{T+1} \nu(\boldsymbol{s}_{T+1}, \boldsymbol{q}_T) \right] \right\} \tag{1.1}$$

subject to :

$$\boldsymbol{s}_{t+1} = \boldsymbol{s}_t + \boldsymbol{q}_t - \boldsymbol{C}_{j,k} r_t - \boldsymbol{e}_t \tag{1.2}$$

$$\boldsymbol{s}_{min} \leq \boldsymbol{s}_{t+1} \leq \boldsymbol{s}_{max} \tag{1.3}$$

$$\boldsymbol{x}_{min} \leq x_t \leq \boldsymbol{x}_{max} \tag{1.4}$$

Where $\boldsymbol{t}$ is time, $\boldsymbol{T}$ is the end of the planning horizon, $\boldsymbol{b}_t$ is a one-stage immediate benefit at stage $\boldsymbol{t}$, $\boldsymbol{x}_t$ is the decision variables (release) vector, $\boldsymbol{s}_t$ is a storage vector at the begin of $\boldsymbol{t}$, $\boldsymbol{q}_t$ are stochastic inflows, $\boldsymbol{e}_t$ are evaporation losses, α is the discount factor, ν is the terminal value function, and E is the expectation operator. $\boldsymbol{C}_{j,k}$ is the connectivity matrix between reservoirs which can be 1 (-1) when the reservoir $\boldsymbol{j}$ receives (releases) water from/to reservoir $\boldsymbol{k}$.

When the objective is maximizing the net benefit from hydropower generation, $\boldsymbol{b}_t(.)$ typically include the economic return from hydropower generation but also penalties for not meeting various operational constraints like minimum flow requirements, spillages losses, etc.

$$\boldsymbol{b}_t = \boldsymbol{HP}_t - \boldsymbol{\xi}_t^{'} \boldsymbol{z}_t \tag{1.5}$$

where$\boldsymbol{z}_t$ is a vector of deficits or surpluses, and $\boldsymbol{\xi}_t^{'}$ is a vector of penalty coefficients (\$/unit of penalty or surplus). The hydropower term $\boldsymbol{HP}_t$ is given by :

$$\boldsymbol{HP}_t = \boldsymbol{\tau}_t \sum\nolimits_j (\boldsymbol{\pi}_t(j) - \boldsymbol{\theta}(j) P_t(j)) \tag{1.6}$$

where $\boldsymbol{\tau}_t$ is the number of hours in period $\boldsymbol{t}$, $\boldsymbol{P}_t$ is a vector of energy values(\$/MWh), and $\boldsymbol{\theta}$ is a vector of O&M cost of hydropower plants (\$/MWh). $\boldsymbol{P}_t$ is the hydropower in a given time step $\boldsymbol{t}$, given by

$$\boldsymbol{P}_t = \boldsymbol{\gamma \eta h}(\boldsymbol{s}_t, \boldsymbol{s}_{t+1}, \boldsymbol{x}_t) \boldsymbol{x}_t(\boldsymbol{s}_t, \boldsymbol{s}_{t+1}) \tag{1.7}$$

Where γ is the specific weight of water, η is the turbine efficiency, $\boldsymbol{h}$ is the net head (function of average storage and release decisions), and $\boldsymbol{x}_t$ is the turbined flow.

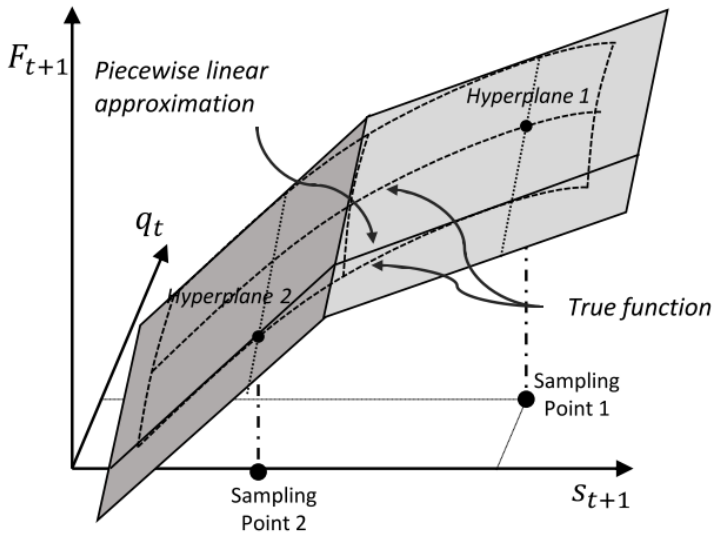

Figure 1.3 – Piecewise linear approximation of benefit-to-go function $\boldsymbol{F}_{t+1}$ (Pina (2017))

1.3 Mid-term model (MT)

Stochastic Dual Dynamic Programming (SDDP) is an extension of Stochastic Dynamic Programming (SDP) that addresses the problem of dimensionality found in SDP (Pereira (1989)). In SDDP, the one stage optimization problem is a LP that maximizes the sum of current $\boldsymbol{b}_t$ and future benefits $\boldsymbol{F}_{t+1}$. The objective function becomes :

$$F_t(\boldsymbol{s}_t, \boldsymbol{q}_t) = \max_{\boldsymbol{x}_t} \{\boldsymbol{b}_t(\boldsymbol{s}_t, \boldsymbol{x}_t, \boldsymbol{q}_t) + \boldsymbol{\alpha}_{t+1}\boldsymbol{F}_{t+1}\} \tag{1.8}$$

We can see that the benefit-to-go $\boldsymbol{F}_{t+1}$ is a scalar.

The scalar $\boldsymbol{F}_{t+1}$ is bounded from above by a set of hyperplanes, which are additional linear constraints approximating the benefit-to-go function :

$$\begin{cases} F_{t+1} - \boldsymbol{\phi}^1_{t+1}\boldsymbol{s}_{t+1} \leq \boldsymbol{\gamma}^1_{t+1}\boldsymbol{q}_t + \boldsymbol{\beta}^1_{t+1} \\ \vdots \\ F_{t+1} - \boldsymbol{\phi}^L_{t+1}\boldsymbol{s}_{t+1} \leq \boldsymbol{\gamma}^L_{t+1}\boldsymbol{q}_t + \boldsymbol{\beta}^L_{t+1} \end{cases} \tag{1.9}$$

where $\boldsymbol{L}$ is the number of hyperplanes, ϕ^l_{t+1}, γ^l_{t+1}, and β^l_{t+1} are the parameters of the $l^{\,th}$ expected cut obtained from the primal and dual variables calculated at stage $t+1$ (Tilmant and Kelman (2007)). In Figure 1.3, hyperplane 1 and hyperplane 2 show the approximated hyperplanes. The linear segments F_{t+1} are obtained from the dual solutions of the optimization problem at each stage and can be interpreted as Benders cuts in a stochastic, multistage decomposition algorithm. SDDP uses an iterative optimization/simulation strategy to increase the accuracy of the solution by adding new cuts.

The hydrologic state variable $\boldsymbol{q_t}$ are the natural inflows observed during the last p periods $\boldsymbol{q_t(j)} = [\boldsymbol{q}_{t-1}(j), \boldsymbol{q}_{t-2}(j), \boldsymbol{q}_{t-3}(j), ..., \boldsymbol{q}_{t-p}(j)]$ and the current inflow is described by a multi-site periodic autoregressive model MPAR(p) :

$$\frac{q_t(j) - \mu_{q_t}(j)}{\sigma_{q_t}(j)} = \sum_{i=1}^{p} \phi_{i,t}(j)(\frac{q_{t-i}(j) - \mu_{q_{t-i}}(j)}{\sigma_{t-i}(j)}) + \xi_t(j) \tag{1.10}$$

where μ_{q_t} and σ_{q_t} are the vectors of periodic mean and standard deviation of q_t, respectively. $\phi_{i,t}$ is the vector of autoregressive parameter of the lag-p periodic model, and ξ_t is a time dependent stochastic noise with mean zero and periodic variance $\sigma^2{}_{\xi,t}$. This model is capable of representing seasonality and serial and spatial inflow dependence within a river basin and among different basins and produce synthetic streamflows scenarios. More details on MPAR(P) can be found in Pina et al. (2017b).

As indicated earlier, the hydropower production function includes the product of the turbined outflow $\boldsymbol{x_t}$ $(\boldsymbol{r_t})$ $(\boldsymbol{m}^3/s)$ with the net head $\boldsymbol{h}(m)$ on the turbine. This brings non-linearity and non-convexity to the first part of Eq. 1.8. Various approaches have been proposed to handle the non-convexity in a LP framework : adding a production coefficient (Archibald et al. (1999)), convex hull approximations (Goor et al. (2011)), Mc-Cormick envelopes (Cerisola et al. (2012)), or a concave approximation (Zhao et al. (2014)).

To deal with the head effects on the hydropower production function Pt , a convex hull approximation is stored in the constraints set (1.11). The linear parameters ψ, ω and δ are determined using the procedure described in Goor et al. (2011).

$$\begin{cases} \hat{P}_t - \boldsymbol{\psi}^1 \boldsymbol{s}_{t+1}/2 - \omega^1 \boldsymbol{r}_t \leq \boldsymbol{\delta}^1 + \boldsymbol{\psi}^1 s_t/2 \\ \vdots \\ \hat{P}_t - \boldsymbol{\psi}^H \boldsymbol{s}_{t+1}/2 - \omega^H \boldsymbol{r}_t \leq \boldsymbol{\delta}^H + \boldsymbol{\psi}^H s_t/2 \end{cases} \tag{1.11}$$

where H is the number of the planes approximating the real hydropower functions ψ, ω, and δ are the parameters obtained from the respective convex hulls.

SDDP is an iterative algorithm that employs two phases to gradually increase the accuracy of the solution by adding new cuts : a backward optimization and a forward simulation. In the backward phase, K inflow scenarios are generated by the MPAR(p) model for each node of the system. These scenarios are applied to calculate the hyperplanes' parameters and to provide an upper bound to the true expected benefit-to-go function (FBF). In the forward phase, the MPAR model generates M synthetic reservoir inflows sequences to simulate the system behaviour over the planning period. This forward simulation phase provides a lower bound that allow us to determine whether the upper bound is a good a approximation or

not. If the upper bound does not fall inside the confidence interval of the lower bound, the approximation is statistically not acceptable and a new backward recursion is implemented with a new set of hyperplanes build on the storage volumes that were visited during the last simulation phase.

At each run of SDDP, the optimal operating policies are simulated over M historical hydrologic sequences of T weeks. T should be chosen so as to be sufficiently long to avoid the effects of the boundary conditions (initial storages and zero terminal value functions) on reservoir operating policies on intermediate years (Goor et al. (2011)). Here, the results are analyzed for the year in the middle which is not affected by the boundary conditions. The main results are weekly storage levels and weekly water values that the latter will guide the daily operations in the ST model.

1.4 Short-term model (ST) and integration with MT

As mentioned earlier, the ST model is based on LP. This choice is motivated by the fact that the ST model must be run a large number of times (number of days times number of members). Hence, computational efficiency is an important criterion. Moreover, since our analysis mostly consists in comparing the production of energy corresponding to different ESF, the approximations associated with the linearization of the objective function should not affect the conclusions.

The objective function Z_{ST}^m of the ST model implemented on the member m can be written as :

$$Z_{ST}^m = \max_{\boldsymbol{x}_d^m} \left\{ \sum_{d=1}^{D} \boldsymbol{b}_d(\boldsymbol{s}_d, \boldsymbol{x}_d^m, \boldsymbol{q}_d^m) + \boldsymbol{\alpha}_{D+1} F_{D+1} \right\} \tag{1.12}$$

where d is the index of day, D is the end of the forecast horizon (here D = 14), $\boldsymbol{q}_d^m$ is vector forecasted flows for day d associated to member m. The second term of Equation 1.12 is the SDDP-derived benefit-to-go function approximated by L hyperplanes :

$$\begin{cases} F_{D+1} - \hat{\boldsymbol{\phi}}_{D+1}^1 \boldsymbol{s}_{D+1} \leq \sum_{d=D-p}^{D} (\hat{\boldsymbol{\gamma}}_d^1 \boldsymbol{q}_d) + \hat{\boldsymbol{\beta}}_{D+1}^1 \\ \vdots \\ F_{D+1} - \hat{\boldsymbol{\phi}}_{D+1}^L \boldsymbol{s}_{D+1} \leq \sum_{d=D-p}^{D} (\hat{\boldsymbol{\gamma}}_d^L \boldsymbol{q}_d) + \hat{\boldsymbol{\beta}}_{D+1}^L \end{cases} \tag{1.13}$$

The daily benefit-to-go functions F_{D+1} are derived from the weekly ones F_{t+1}. More specifically, for any day $D+1$ in week t, F_{D+1} is interpolated from the neighbouring weekly benefit-to-go function F_t and F_{t+1} (Figure 1.4). In other words, the parameters ($\hat{\boldsymbol{\phi}}$, $\hat{\boldsymbol{\gamma}}$, $\hat{\boldsymbol{\beta}}$) of the hyperplanes associated with F_{D+1} are linearly interpolated from the parameters ($\boldsymbol{\phi}$, $\boldsymbol{\gamma}$,

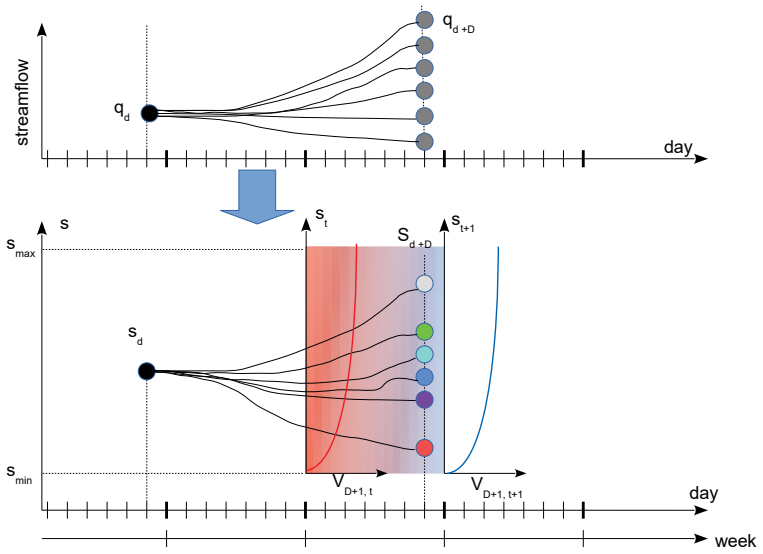

Figure 1.4 – Implementing mid-term water values into short-term model

$\boldsymbol{\beta}$) corresponding to the weekly functions F_{t+1}. This interpolation procedure ensures that the benefit-to-go function is available at the end of each day.

In the ST model, the non-convexity of the hydropower function is addressed using the same approach as in the MT model, i.e with the same convex-hulls.

$$\begin{cases} \hat{P}_d - \boldsymbol{\psi}^1 \boldsymbol{s}_{d+1}/2 - \omega^1 \boldsymbol{r}_d \leq \boldsymbol{\delta}^1 + \boldsymbol{\psi}^1 s_d/2 \\ \vdots \\ \hat{P}_d - \boldsymbol{\psi}^H \boldsymbol{s}_{d+1}/2 - \omega^H \boldsymbol{r}_d \leq \boldsymbol{\delta}^H + \boldsymbol{\psi}^H s_d/2 \end{cases} \tag{1.14}$$

Note that in the current version of the ST model, the travel time between two consecutive power plants is ignored.

1.5 The rolling-horizon approach

Basically, the rolling horizon approach is based on three steps that are repeated every day over the planning period : (1) based on the current status of the system (storage levels, past weekly inflows, and updated ESF, determine the optimal release decision for day d, (2) implement that release decision and assess storage level at the end of the day (s_{d+1}), (3) update the storage s_{d+1} with the actual inflow q_d.

The release decision made at the beginning of day d must be chosen from a set of M optimal decisions, one per member, identified by the ST optimization model. Here, the actual decision

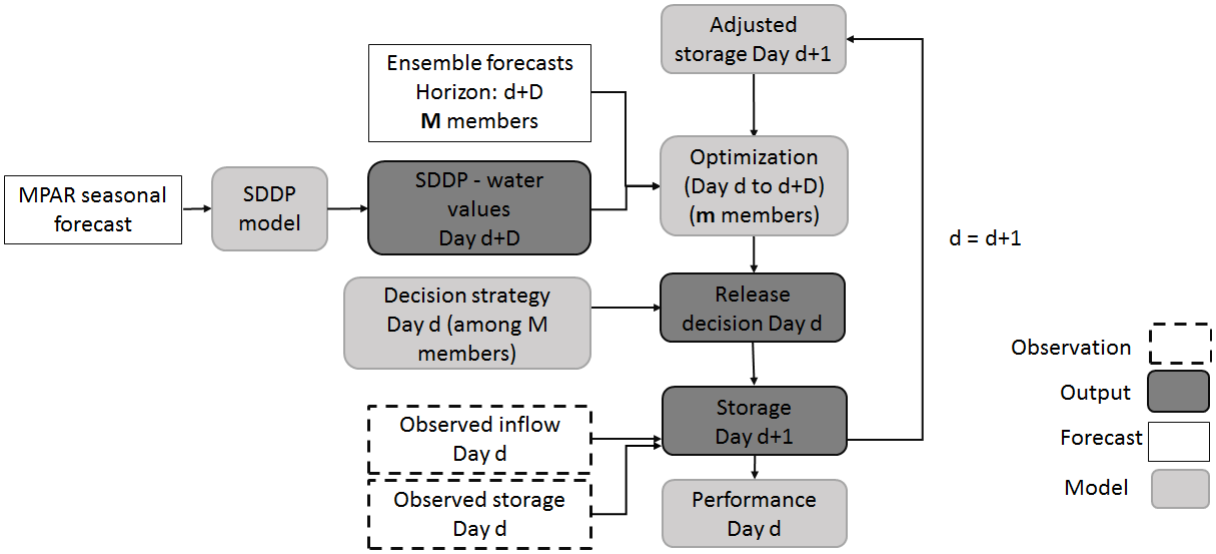

Figure 1.5 – The structure of the combined short- and mid-term operational model based on rolling horizon

r_d is the mean of all decisions :

$$r_d = \frac{1}{M} \sum_m r_d^m \tag{1.15}$$

where $r_{d,m}$ is the decision associated with the m^{th} member.

At the beginning of the next day (d+1), the simulated storage s_{d+1} is calculated from s_d, the actual release r_d and the actual (observed) flow $\boldsymbol{q}_d$:

$$\boldsymbol{s}_{d+1} = \boldsymbol{s}_d + \boldsymbol{q}_d - \boldsymbol{C}\boldsymbol{r}_d - \boldsymbol{e}_d \tag{1.16}$$

This process is repeated each day until the end of the operation horizon (OH) is reached. The main results are time series of daily hydroelectric productions, storage levels, turbined outflows and spillages losses. Figure1.5 displays the structure of the MT-ST model based on rolling horizon approach.

Chapitre 2

Case study

The Gatineau River in Quebec is one of the main tributaries of the Ottawa River. The river drains an area of 23,700 km^2. The hydroelectric system consists of a cascade of four power stations and two large reservoirs (Figure 2.1). The flow regime is highly regulated by two upstream reservoirs : Cabonga and Baskatong. Baskatong supplies water to the Mercier power plant whose outflows are then used to spin the turbines of three run-of-river power stations : Paugan, Chelsea and Rapid Farmers. Paugan is a run-of-river power plant (R-O-R) with a total capacity of 219 MW and a small reservoir of 30 km^2. Chelsea and Rapides Farmer have an installed capacity of 149 MW and 95 MW respectively. Table (2.1) lists the main characteristics of the system. As we mentioned before, the Gatineau River basin comprises inhabited areas and the main operating concerns are hydropower production. Apart from that, the Baskatong reservoir must be kept high from 1 June to 15 September, to allow boating and recreational activities for nearby residents. Moreover, the river level must be kept above a specific level to ensure adequate drinking water supply for nearby towns. Finally, the river must also be kept low for flood risk. The average volume of a spring flood in the Baskatong reservoir is higher than the capacity of the Baskatong reservoir. The routine strategy is to lower the level of the Baskatong reservoir at the end of the winter as much as possible and then let the level rise during spring. Then, the reservoir level is kept all summer within 2.5 to 1.3 m of its maximum level until mid-September. During the fall, the reservoir is managed so that a sufficient water reserve is cumulated to anticipate electricity demand during winter. The operating margin for the operation of the Baskatong reservoir is quite small considering the above mentioned constraints and the inflows it receives during certain periods. Consequently, spillage is sometimes inevitable at the hydropower stations in spring and fall. The most significant flood occurred in the spring of 1974. On this occasion, 3000 residents were required to evacuate the area, over one-third of Maniwaki (downstream of Baskatong) was flooded and 2.9 million Canadian dollars had to be provided in disaster relief.

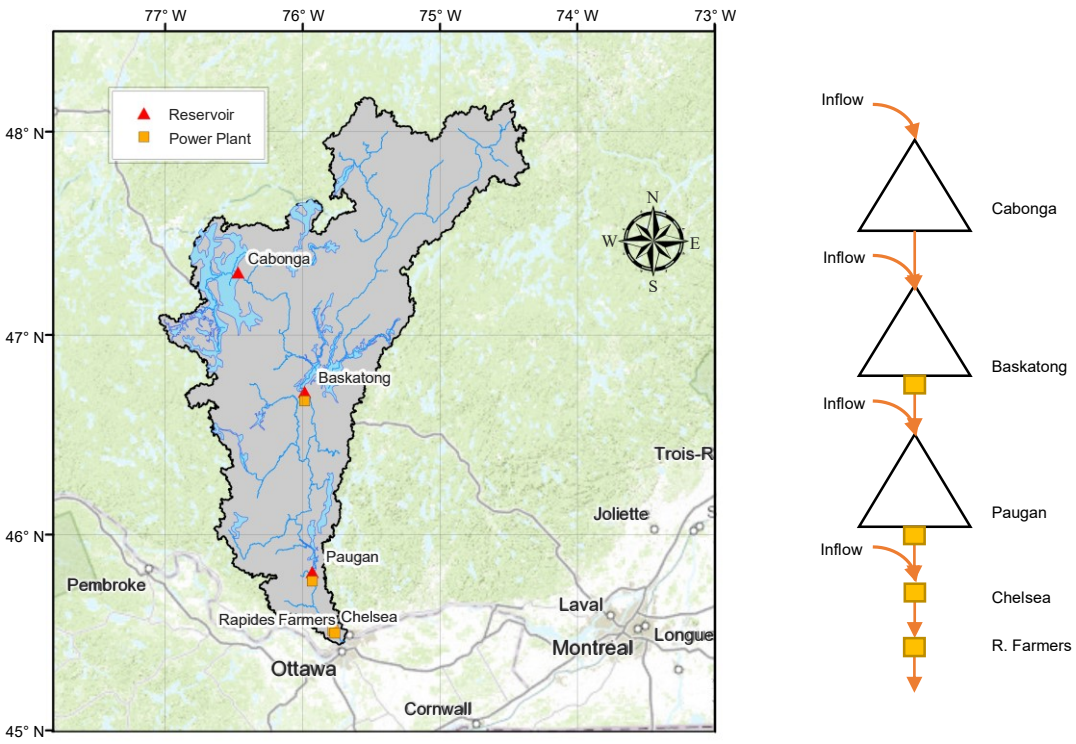

Figure 2.1 – Gatineau River Basin (Pina et al. (2017b))

Node	Name	Storage Hm^3	Installed Capacity MW
1	Cabonga	1633	-
2	Baskatong	3175	50
3	Paugan	93	219
4	Chelsea	ROR	148
5	Rapides Farmers	ROR	95

[a] ROR : Run of the river power plant

Table 2.1 – hydropower system of Gatineau River basin

2.1 Ensemble streamflow forecasts for the Gatineau River basin

The ensemble streamflow forecasts (ESF) for the Gatineau river basin have been generated by F. Anctil's group at U. Laval. The starting point are ensemble meteorological forecasts produced by the European Center for Medium range Weather Forecasts (ECMWF) (Fraley et al. (2010)). These 50 ensemble forecasts are produced over a 14-day horizon and with a temporal resolution of 12 hours.

Then, they are used as inputs to 20 lumped hydrologic models. The models are selected by Seiller et al. (2012) based on their performance and structural diversity, i.e. 4 to 10 free param-

eters, and 2 to 7 storage units. The structure of all hydrologic models include some conceptual storages (see Figure 2.2) to describe the main hydrological processes. All models implement a time-delay function for routing ; they also consider the physical characteristics of the catchments using a parametric logistic function. Snow accumulation and snow melting are computed externally. They are all designed to take into account soil moisture with various linear and non- linear formulations. Figure 2.2 summarizes the structure of the 20 models. The models exhibit low to moderate complexity (four to ten free parameters and two to seven storages). The input data for the lumped models are precipitation and potential evapotranspiration. A more detailed illustration of the models can be found in Perrin (2000) and Seiller et al. (2012).

In this case study, each hydrological model is applied on the four sub-basins generating the incremental flows in the system (Figure 2.1). Together, these 20 hydrologic models capture the structural uncertainty associated with the modeling of the relevant hydrologic processes.

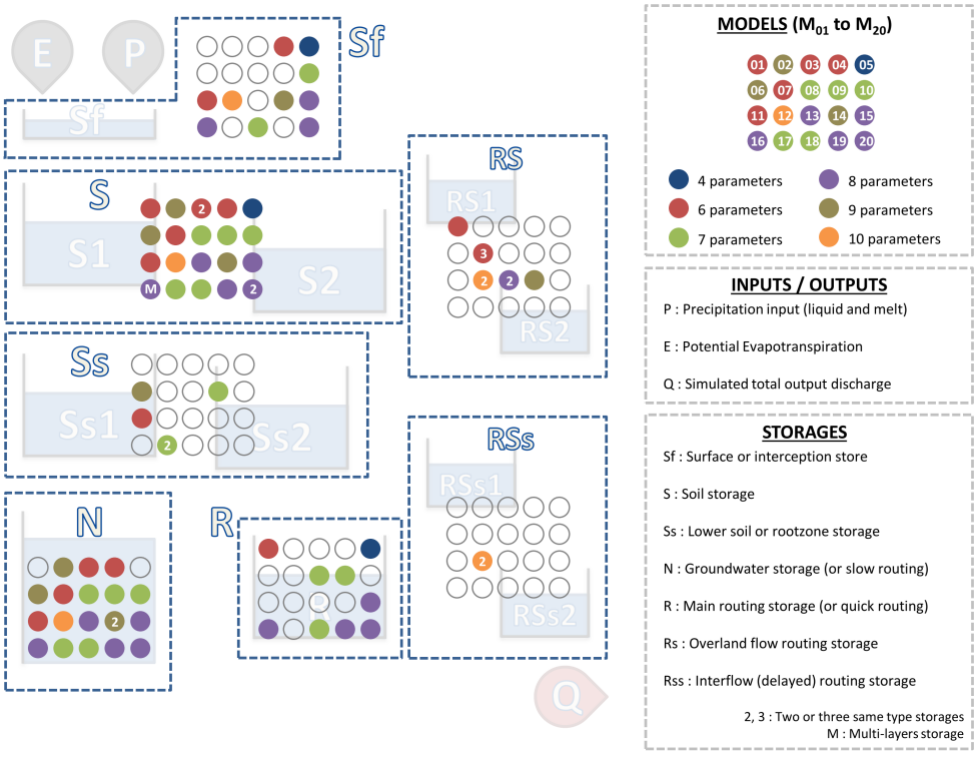

Figure 2.2 – structure of 20 hydrologic models (from Seiller et al. (2012))

To capture the uncertainty attached to the initial (hydrologic) conditions, Ensemble Kalman Filter (EnKF) is employed to create an ensemble of 50 possible initial conditions based on the true probability density function of the model states conditioned by the observations. Hence, for each hydrologic model, an ensemble of 2500 members is produced. Because the computational burden associated with the ST model is directly proportional to number of members, the size is reduced to 50 by randomly selecting one out of the 50 EnKF initial conditions. In the end, each hydrologic model produces ESF with 50 members over a 14-day

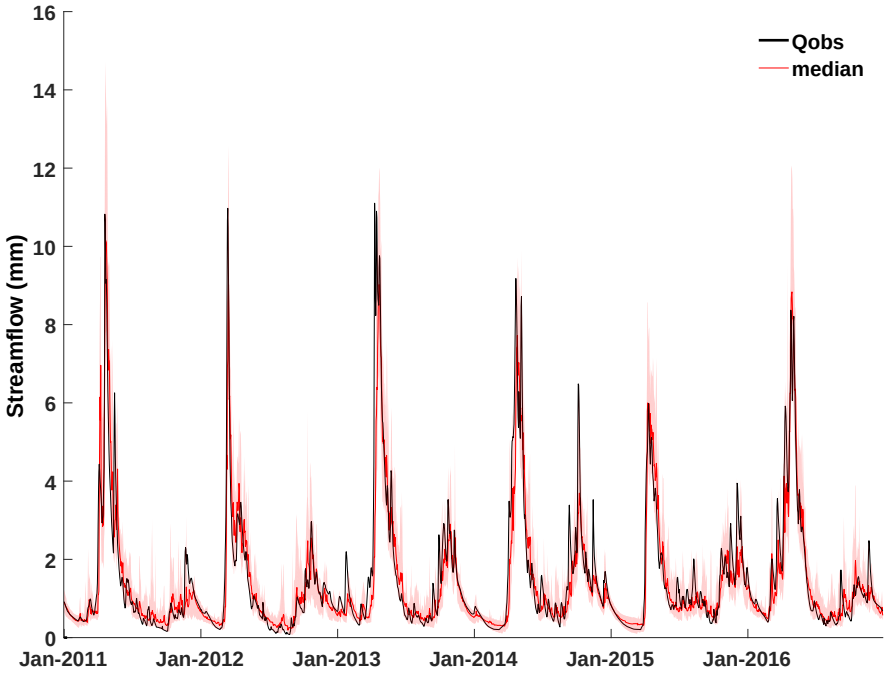

Figure 2.3 – ESFs of Baskatong reservoir from 20 individual hydrologic models for 50 ensemble members (leadtime14 days)

horizon. For the sake of this study, the forecasts are aggregated on a daily time step. Figure 2.3 shows the daily ESFs for the Baskatong reservoir.

2.2 SDDP for the Gatineau River basin

The SDDP model is coded in MATLAB and the optimization scheme uses the linear Gurobi solver. The model is implemented with 30 backward openings (K=30) and 35 hydrologic sequences derived from the built-in MPAR(1) (M=35). The planning period of the mid-term model is 5 years (T=260 weeks), but the results are analyzed for year three only as the first and last two years are influenced by the boundary conditions (years 1 and 2 for the initial conditions, and years 4 and 5 for the terminal conditions). The SDDP-derived future benefit function approximations (F_{t+1}) from the third year (t = 105,...,157), are then passed on to the short-term model.

Figure 2.4 displays the marginal water value (panel a) and drawdown refill cycle (panel b) of the Baskatong reservoir. In general, during the first weeks of the year (winter season), water values decrease and the storage draws-down to deplete the reservoir for the following floods during the snowmelt season (weeks 12-24). During this period, the water values increase and the storage is refilled.

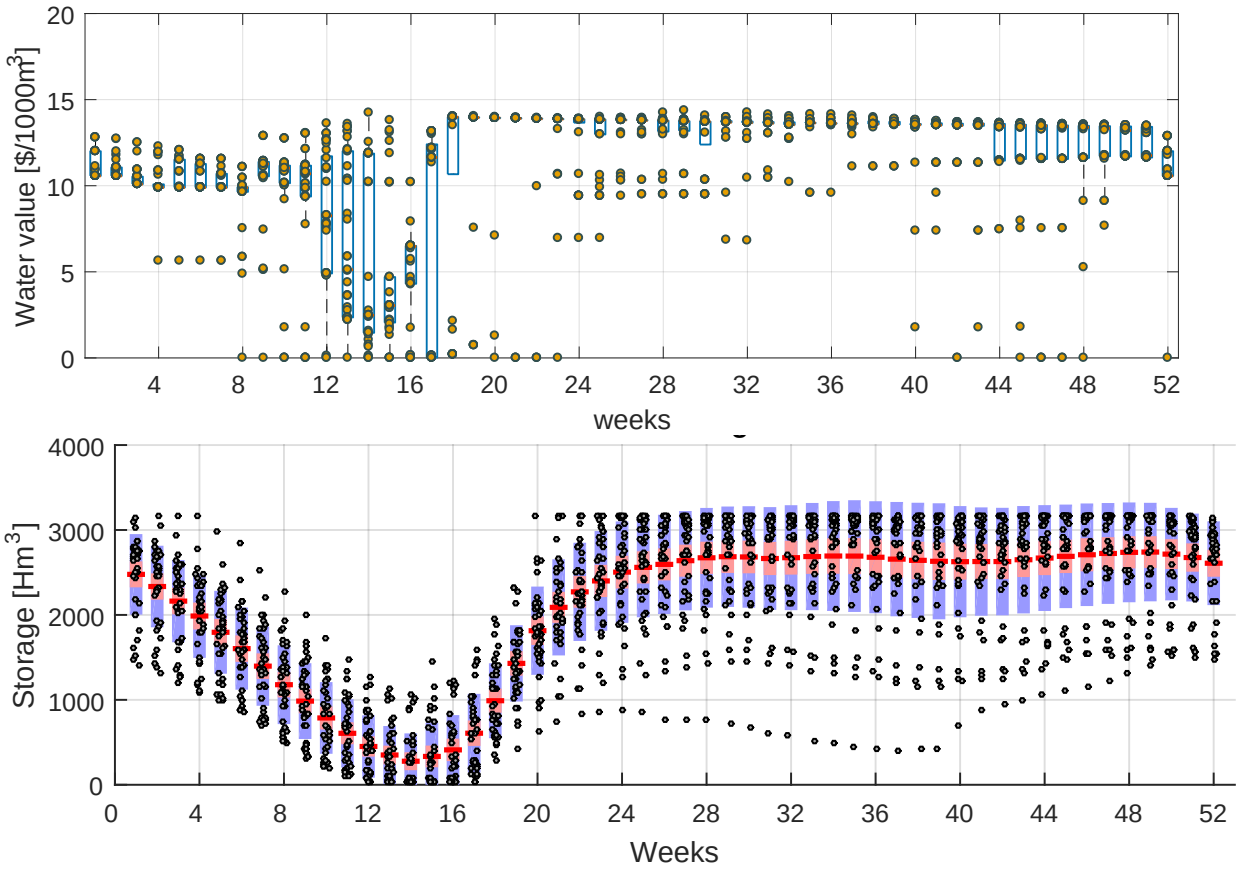

Figure 2.4 – SDDP derived marginal water value (panel a) and optimal storage of Baskatong reservoir(panel b) (35 years)

2.3 LP for the Gatineau River basin

The LP model for the Gatineau river system is also coded in MATLAB and also uses the Gurobi solver (see Appendix). The first input are the 14-day ESFs (FH = 14) with 50 members, which are available for 20 hydrologic models over an operation horizon (OH) of 6 years. Another input are the daily SDDP-derived benefit-to-go functions, which are available as a set of coefficients $\hat{\boldsymbol{\phi}}$, $\hat{\boldsymbol{\gamma}}$, and $\hat{\boldsymbol{\beta}}$.

To better perceive the impact of the structural uncertainty associated with the hydrological models on the performance of the system, the problem was solved based on two configurations. In the first configuration, the reservoir operation problem is solved individually for each hydrological model. In other words, the rolling-horizon approach is implemented 20 times, one per hydrologic model, yielding a total of 2,192,000 LP model runs : 50 ESF members $\times$ 2192 days $\times$ 20 hydrologic models. The main outputs therefore consist of 20 time series of optimal release decisions, hydroelectric productions, storage levels, and spills over 2192 days.

In the second configuration, the rolling horizon approach is implemented once, aggregating the results of all hydrologic models. Here, the actual decision at day d, is the average over the

50×20 decisions associated with the pairs (member - hydro model). In this configuration, we assume that the pairs (member - hydro models) are equally-likely ; that is, the pairs have the same weight. The outputs here are (single) time series of hydroelectric production, storage levels, releases, and spills.

Chapitre 3

Analysis of simulation results

Figure 3.1 shows the average drawdown-refill cycle of the Baskatong Reservoir for the first and second configuration. As observed in this figure, the drawdown starts in the summer and continues until days 77-78 when the snowmelt season begins. The reservoir then quickly refills at the beginning of the following summer. For the second configuration, as expected, we can see that the optimal storage lies within the zone defined by the trajectories identified with the first configuration (20 hydro models separately).

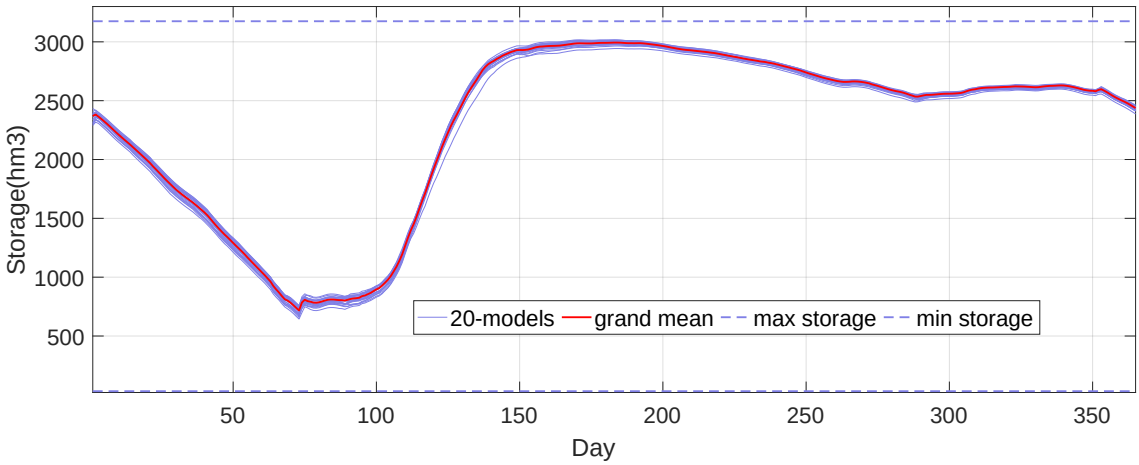

Figure 3.1 – Optimal short-term storage levels for Baskatong reservoir for 20 hydrologic models (first configuration) and grand mean (second configuration)

With the first configuration, the optimization framework yields 20 time series of daily energy at each power plant, each corresponding to a particular hydrologic model. To measure how well the hydrologic models perform, a comparison is made between the energy generated with the individual ESFs and the perfect forecasts (PF) (i.e. when the forecasted flow is replaced by the observed flow). In other words, the benchmark is the energy generated in a semi-deterministic environment in which the short-term hydrologic uncertainty is ignored. The normalized difference between the energy generated with the ESF and the PF is the

performance indicator used in this study. Let $\Delta^h(j)$ be the relative difference between the energy generated at the power plant j with PF and with ESF corresponding to the hydrological model h :

$$\delta^h(j) = \frac{\Delta^h(j) - min(\Delta^{\cdot}(j))}{max(\Delta^{\cdot}(j)) - min(\Delta^{\cdot}(j))} \tag{3.1}$$

The closer $\delta^h(j)$ is to zero, the closer is the energy generated with model h to the energy generated with PF. Conversely, the hydrologic model with $\delta^h(j)$ approaching 1 shows the largest energy difference with respect to the perfect forecast and therefore performs poorly in economic/utility terms.

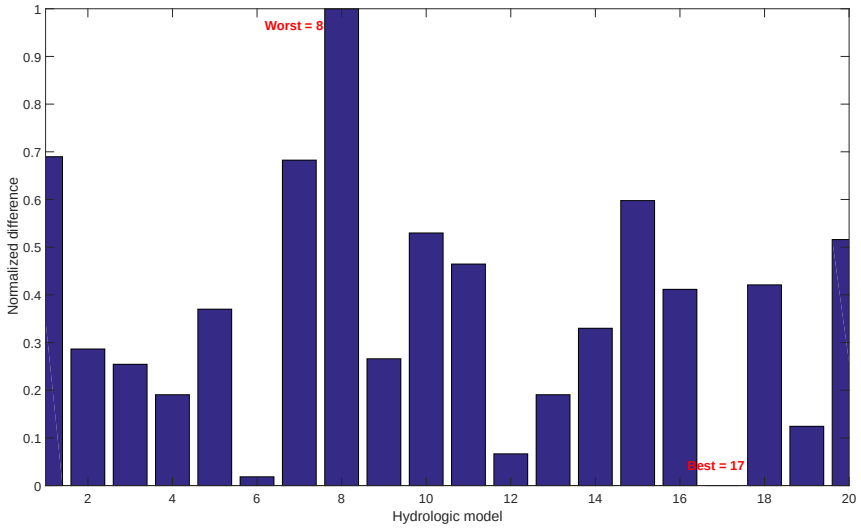

Figure 3.2 – Energy performance of 20 hydrologic models over 6 years for Gatineau River basin

Figure 3.2 displays the performance of 20 hydrologic models for the Gatineau River basin during the operation horizon (OH = 6 years). The x-axis represents 20 hydrological models, while the y-axis is the performance indicator (δ) of the models. It is important to note that the generated energy at the power plant located in the outlet of the basin is the aggregated energy of that power plant and the upstream power plants. Therefore, the energy performance at this power plant (R-Farmers) is representative of the basin-wide energy performance. The best performance is achieved with M_{17}, while the worst is observed with M_{08}. Table 3.1 shows that M_{17}, M_{06}, M_{12} outperforms the others. Since the optimization formulation and the benefit-to-go functions' parameters were the same for all 20 runs, the forecasts' quality appears to be the only factor responsible for those differences.

The probabilistic hydrological forecasts are assessed in terms of accuracy, resolution and reliability. An ensemble streamflow forecast can be considered reliable if it contains all of the observations within the uncertainty bounds ; however, if the uncertainty bounds are very large,

Ranking	energy performance
1	M_{17}
2	M_{06}
3	M_{12}
4	M_{19}

Table 3.1 – The best four models in terms of energy generation for Gatineau river basin

the precision of the ensemble becomes low and the ensemble is not useful for decision-making purposes. For instance, a reliable 80% confidence interval should contain the observation eight times out of 10 on average. Resolution evaluates the ability of discriminating between two events which are different. Accuracy is a measure of the distance between forecast and observation. Traditional deterministic scores like mean absolute error (MAE) cannot be used in order to measure the quality of the probabilistic forecasts. The quality of the probabilistic forecasts are often characterized by the continuous ranked probability score (CRPS ; Matheson and Winkler (1976)), which assesses the accuracy of the ensemble forecasts. It is defined as :

$$\boldsymbol{C}RPS(F_t, x_{obs}) = \int_{-\infty}^{+\infty} (F_t(x) - H(x \geq x_{obs})^2 dx \tag{3.2}$$

where $F_t(x)$ is the cumulative distribution function at time t, x is the predicted variable, and x_{obs} is the observed value. The function H is the Heaviside function, which equals 0 for the predicted values less than the observed value, and 1 for the values greater than the observation. Figure 3.3 shows the relationship between the quality of the forecasts and performance of the hydropower system for each power plant. The forecasts are characterized by the CRPS while the performance is illustrated by the indicator δ i.e. the normalized difference between the energy generated with PF and ESF. Because the CRPS are available for each sub-basin, the scores must be aggregated. In this case, the aggregation is simply the average of the upstream CRPS associated with the sub-basins drained by the power plant. Despite this approximation, it can be clearly observed that the hydrologic models with the low CRPS tend to perform better. In the upstream reach (Baskatong), models M_{13} and M_{05} appear to be the most interesting ones. Further downstream, at Paugan, the group is extended and now includes models M_{12}, M_{17}, M_{09} and M_{06}, which are again found at Chelsea. M_{09} in Paugan is replaced by M_{19} in Chelsea. The least interesting models are either M_{07} or M_{08} depending on the site.

Table 3.2 provides a ranking of the most interesting hydrologic models and their structure. As we can see, all of the models include soil storage (S) and groundwater storage (N) in their structure. Apart from M_{12}, none of the models incorporate surface storage (Sf). Among the 20 models, M_{17} and M_{06} are among the few models that have a root zone storage (Ss) component. Among the models with better performance, M_{19} is the only one that employs main routing storage (R) in the structure. Moreover, M_{12} and M_{13} are among the few models that apply overland flow storage (RS) with two storages in their structure. Interestingly, M_{12}, which is

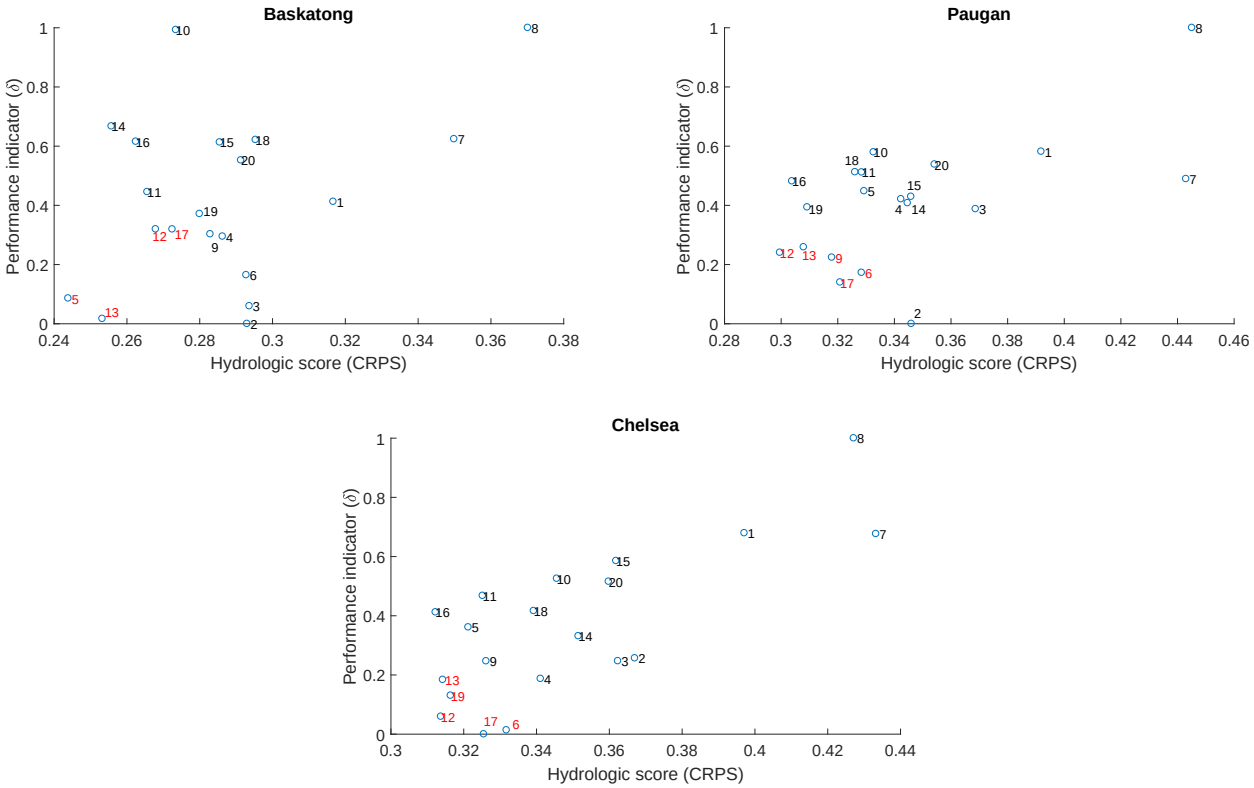

Figure 3.3 – the relationship between the performance of the models and their hydrological scores (three sub-basins)

	S	N	Sf	Ss	R	Rs	RSs	Free calibrated parameters
M_{12}	*	*	*	-	-	*	*	10
M_{13}	*	*	-	-	-	*	-	8
M_{06}	*	*	-	*	-	-	-	9
M_{17}	*	*	-	*	-	-	-	7
M_{19}	*	*	-	-	*	-	-	8

* = The element present in the model
S = soil storage ; N= groundwater storage
Sf = surface storage ; Ss = root zone storage
R = quick routing storage ;
Rs = overland flow routing storage ;
RSs = interflow routing storage

Table 3.2 – The structure of the best models during the operation horizon (OH=6 years)

the most complex model with seven storages and ten free calibrated parameters, is the only model that employs interflow routing storage (RSs) with two reservoirs.

Table 3.3 provides the structure of the models which perform poorly. Likewise, it is unclear which components of M_{07} and M_{08} lead them to perform poorly. Apart from the common structure (incorporating S and N) of these two models compared to the other models, M_{08}

	S	N	Sf	Ss	R	Rs	RSs	Free calibrated parameters
M_{07}	*	*	-	-	-	*	-	7
M_{08}	*	*	-	-	*	-	-	7

* = The element present in the model
S = soil storage; N= groundwater storage
Sf = surface storage; Ss = root zone storage
R = quick routing storage;
Rs = overland flow routing storage;
RSs = interflow routing storage

Table 3.3 – The structure of the worst models during the operation horizon (OH=6 years)

uses a linear R which may cause poor performance of this model among the others. M_{07} also applies three RS and incorporates six free calibrated parameters.

Generally, the models that incorporate more than six free calibrated parameters always perform better, while the models that include Sf and R do not perform well. However, M_{12} and M_{19} are exceptions, which include Sf and R in their structures and they are in the group of the models with good performance.

The Gatineau River basin is characterized by a warm and humid climate during the summer, and generally wet, cold and snow-covered in the winter. This climate leads to very high flows during spring-summer (i.e. snowmelt season; weeks 11-24). To consider the impact of seasonality, the average of the six years performance indicator (δ) and CRPS during the snowmelt season (days 77-168) and the rest-of-the-year (days 1-77 and days 169-365) are calculated for 20 hydrologic models. Figures 3.4 and 3.5 display the relationship between the performance of the hydropower (δ) for each power plant (y-axis) and the quality of the forecasts (CRPS) (x-axis) during the periods of snowmelt and rest-of-the-year, respectively.

Figure 3.4 illustrates that during the snowmelt season, M_{05} and M_{13} appear to possess better energy performance and CRPS for the upstream power plant (Baskatong). However, by moving to the Paugan, the group extends to M_{12} and M_{16}. In the downstream power plant (Chelsea), M_{11} joins this group. Figure 3.5 shows that during the rest-of-the-year period, apart from M_{05} and M_{13} that still appear interesting, M_{06} also performs well in the upstream reach (Baskatong). By moving downstream (Paugan), M_{05} leaves and M_{12} and M_{17} join this group. In the downstream power plant (Chelsea) M_{19} joins the group.

Comparing Figures 3.4 and 3.5 reveals that some of the models perform well in both periods of the snowmelt season and rest-of-the-year. For instance, M_{05} and M_{13} for the upstream power plant (Baskatong) and M_{12} and M_{13} for the downstream power plant (Chelsea) perform well in both periods. However, some models perform differently during the two periods. For example, during the snowmelt season, M_{05}, M_{11}, and M_{16} are among the interesting models for

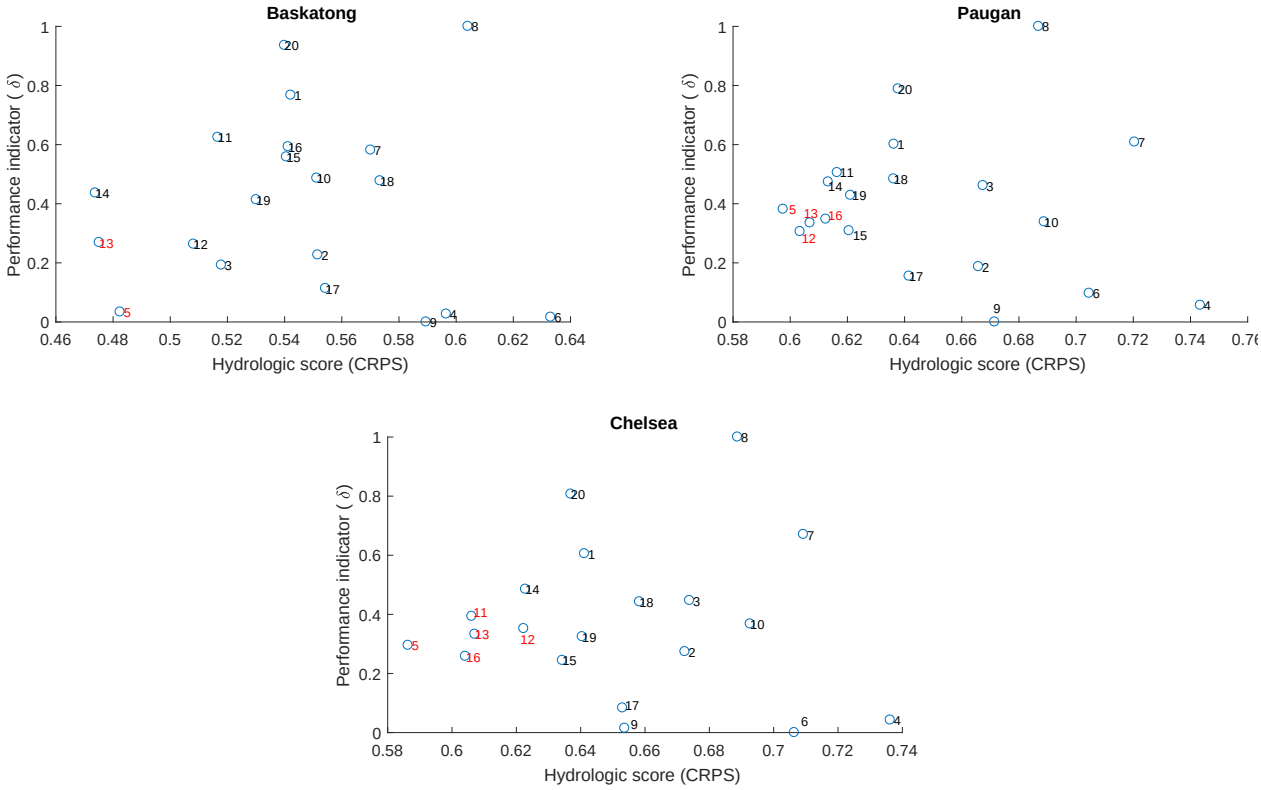

Figure 3.4 – the relationship between the performance of the models and their hydrological scores (three sub-basins) - snowmelt season

the downstream power plant ; however, during the rest-of-the-year period, M_{06}, M_{17}, and M_{19} appeared to possess better performance. It is important to note that the best models during the operation horizon (OH=6 years) (Figure 3.3) and during the rest-of-the- year period (3.5) for the downstream power plant are similar. Thus, the analysis structure of the best models during the rest-of-the-year period is the same as the operation horizon (Table 3.2).

	S	N	Sf	Ss	R	Rs	RSs	Free calibrated parameters
M_{12}	*	*	*	-	-	*	*	10
M_{13}	*	*	-	-	-	*	-	8
M_{05}	*	-	*	-	*	-	-	4
M_{11}	*	*	*	*	-	-	-	6
M_{16}	*	*	*	-	*	-	-	8

* = The element present in the model
S = soil storage ; N= groundwater storage
Sf = surface storage ; Ss = root zone storage
R = quick routing storage ;
Rs = overland flow routing storage ;
RSs = interflow routing storage

Table 3.4 – The structure of the best models during the snowmelt season

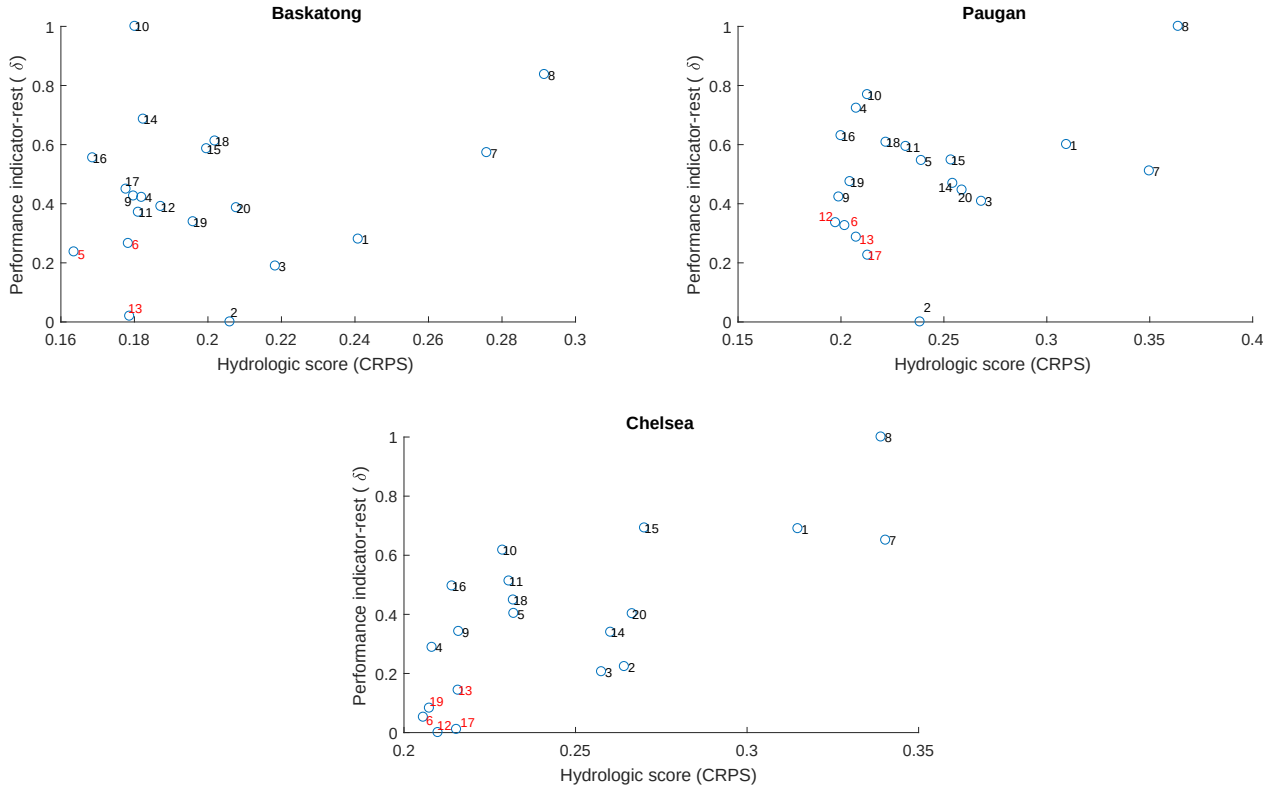

Figure 3.5 – the relationship between the performance of the models and their hydrological scores (three sub-basins) - rest of the year

Based on Figures 2.2 and 3.4, the structure of the best models during the snowmelt season for the Gatineau River basin is presented in Table 3.4. As observed, all the best models incorporate N and S, which are the common characteristics of all hydrologic models ; however, M_{05} is an exception, because it is the simplest model with only four calibrated parameters, and the only model that does not include N in the structure.

As observed in Table 3.4, all the best models include Sf in their structure ; however, M_{13} is an exception, which does not incorporate Sf. M_{11} is the only model that includes Ss, with six free calibrated parameters. M_{05} and M_{16} are the models that incorporate R in their structure. This might suggest that quick routing storage (R) helps the models to perform well during the snowmelt season.

M_{12} and M_{13} are the models which perform well during both the snowmelt and rest-of-the-year periods. Among all 20 models, they are the few that incorporate RS in their structure. It was previously mentioned that M_{12} is the most complex model with 10 calibrated parameters and the only model that includes RSs in the structure. In the both periods (snowmelt and rest-of-the-year), M_{07} and M_{08} appeared to perform poorly.

As observed in Table 3.4, Sf is the element which appeared in the structure of most of the

models with good performance during the snowmelt season ; however, the best models during the rest-of-the-year period (Table 3.2) do not incorporate this element in their structure. It is suggested perhaps with the high amount of surface flow, Sf helps the model to perform better during the snowmelt season.

Similarly, R appeared in the structure of two models during the snowmelt season (Table 3.4) ; however, during the rest-of-the-year period (Table 3.2), this element is observed in the structure of only one model. It maybe suggest that R is more applicable, during the high flow season with more floods.

It is also observed that M_{05} performs well without the incorporation of N in the structure. This suggests that during the high flow season, the groundwater storage for the basin is negligible. More information about the physical characteristic of the basin such as the type of the soil, slope, and land-use will help to better understand the reasons for the high performance of M_{05} during the snowmelt season. However, it is not within the scope of this study to explore the details related to the structure of the models. Furthermore, information regarding the characteristics of the basin such as types of storage (e.g. surface storage, soil storage, routing storage) was not available in this study.

A comparison of Figures 3.4 and 3.5 demonstrate that the values of CRPS for all three reaches during the snowmelt season are higher than the rest of the year. However, this should not be interpreted as the quality of the forecast being lower during the snowmelt season due to CRPS being typically greater for higher flow periods.

	Perfect Forecast	M_{12}	M_{08}	Second configuration
Annual average	2852	2813	2764	2800
Difference	-	% -1.4	%-3.1	%-1.9

Table 3.5 – Annual average energy generation by perfect forecast, second configuration, the best and the worst hydrologic models (GWh/year)

In absolute terms, based onFigure 3.3, the best model (M_{12}) produces 1.7% more energy than the worst model (M_{08}) (see Table 3.5). The annual potential gain of the best model is 3.4 million dollars more than the worst model. The opportunity cost of the best hydrological model corresponds to 1.4% of the amount of energy that could be generated if perfect forecasts were available for the next 14 days. In other words, the lack of perfect foresight reduces the energy output by 1.4% when the best forecasts are utilized. This amount of energy is equivalent to approximately 2.8 million dollars per year. This 3.1% reduction amounts to approximately 6.1 million dollars per year when the worst forecasts are processed by the optimization framework.

When the second configuration is implemented (i.e. the actual decision is the average of the overall models and members), the reduced energy output reaches 1.9% compared to the perfect forecasts, which is 0.5% lower than the amount of energy obtained with the best hydro model

(M_{12}). The potential annual gain of the second configuration is 3.6 million dollars less per year than the perfect forecast and 905 thousand dollars less than the best hydrologic model. This result seems to indicate that the design of a multi-modeling framework for hydrologic forecasting would benefit from a selection of the models based on both their structure and economic performance. For instance, in our case, a group of the models M_{06}, M_{12}, M_{17}, M_{13}, and M_{19} (see Figure 3.3) benefit from the highest energy performance and hydrological scores. Implementing a group of these models, instead of using all 20 hydrologic models, will increase the economic benefits of the daily release decisions that lead to enhancing the benefits of the system.

Chapitre 4

Conclusion and future work

This study presents a modeling framework to optimize the production of hydroelectricity while taking into account short (daily) and mid-term (weekly) forecasts. The framework is used in simulation to analyze the relationship between the quality of the short-term forecasts and their economic performance. This is illustrated using the hydropower system of the Gatineau River basin where ESF, corresponding to twenty hydrologic models, is available on a daily time step over a period of six years. The twenty models capture the structural uncertainty associated with hydrological modeling and therefore, generate forecasts with contrasted quality. Each set of ESF associated with a particular hydrologic model is then processed by the optimization framework to determine the optimal amount of energy that can be generated by the system.

The optimization is repeated 20 times in order to have a sample large enough to analyze the relationship between the quality of ESF and economic performance of the power system. These results confirm that the forecast accuracy tends to improve the performance of the system ; however, the relationship is not univocal. Some hydrologic models may be characterized by a good statistical score, but perform poorly in terms of energy generation.

Considering the economic gains from the models with the best performance, worst performance, and average of all 20 models (second configuration), it can be concluded that applying a group of models with higher performance will increase the benefits of the system. This group of models can be regarded as the basis of a multi-modeling framework. However, the members in the group of the best models change during the snowmelt season.

Because the Gatineau River basin is characterized by high flows during the spring and early summer, the impact of seasonality must be considered. Thus, the relationship between the quality of ESF and economic performance of the system during the snowmelt season is examined. The results show that some of the models that previously appeared in the group of the best models perform differently during the snowmelt season. This implies that the performance of some models is affected by the seasonality, which might affect the design of the multi-modeling framework. In terms of reservoir operation, choosing hydrologic forecasts with

better performance during the snowmelt season is essential as it affects the refill phase of the reservoirs.

To better perceive the impact of structural uncertainties associated with the hydrological models, and as an operational scenario, the second configuration was implemented where the actual decision is the average of all members and all hydro models. The results suggest that the benefits of the system can increase if a carefully chosen subset of hydro models is assembled, but it would require going beyond the mere assessment of the scores and also investigate the economic performance, a process that will likely be more time-consuming.

The short-term optimization can be improved by substituting LP by non-linear programming (NLP) to better handle the non-linearity of the hydropower production function. Future work may also consider the incorporation of travel time between the power plants. It may also be better to have ESF for the total flow at the dams instead of incremental flows in order to facilitate the treatment of the CRPS, which must be aggregated in order to have one score per dam.

Since the optimization formulation and FBF parameters are the same for all 20 hydrologic models, the quality of the forecast is the only factor responsible for the differences in terms of energy output. In this study, we considered CRPS as an indicator of accuracy for the hydrologic forecast. However, future work may consider Nash–Sutcliffe Efficiency (NSE) as another criterion to design multi-model ensemble hydrologic forecasts.

Chapitre 5

Appendix : ST model code in MATLAB

```
% Update day: 2018_10_04
% This code is the daily linear optimization for Gatineau River basin
% to work with the code, the functions Weekly_2_Daily1.m , In_data.m,
% EnergyFun_convHull.m, weekly_2_Daily_Power_Price are required.
%%%%%%%%%%%%%%%%%%%%%%%%%%%%%%%%%%%%%%%%%%%%%%%%%%%%%%%%%%%%%%%%%%%%

clear all;
warning off;
tic;
update= datetime('now');

load('new_Inflow_rand');                                    %The hydrologic Ensemble file
new_Inflow = new_Inflow_rand;
load('Gatine16.mat');
Gatineau{1}=Gatin16{3};
addpath('C:\gurobi652\win64\matlab\')
J=5;                                                        % number of nodes
Ens_hr=size(new_Inflow.new_Inflow(1).new_Inflow.ESF(1, 1).ESF,1);   % forecast horizon
number_of_Years =round(length(new_Inflow.new_Inflow(1).new_Inflow.ESF)/365+1);  %operation years + 1 year = for converting weekly
```

```
    SDDP to daily
operation_horizon = length (new_Inflow.new_Inflow(1).new_Inflow.ESF
    ); %operation horizon

start_Day =1;
end_Day = operation_horizon; %operation horizon
members =size(new_Inflow.new_Inflow(1).new_Inflow.ESF(1, 1).ESF,2);
     % ESF members
% members=1;                    %Perfect forecast
number_of_hydro_models = length(new_Inflow.new_Inflow);
%% Approximation of parameters for energy production coefficient [
    MW/hm3/month]
%CONVEX-HULL
[b_Ca, ~, ~, HPhull_grid_Ca,HPreal_Ca] =EnergyFun_convHull(Gatineau
    {1}.system, 0, 0, 1, 5);  %Cabonga
[b_Ba, ~, ~, HPhull_grid_Ba,HPreal_Ba] =EnergyFun_convHull(Gatineau
    {1}.system, 0, 0, 2, 5);  %Baskatong
[b_Pa, ~, ~, HPhull_grid_Pa,HPreal_Pa] =EnergyFun_convHull(Gatineau
    {1}.system, 0, 0, 3, 5);  %Paugan
[b_Ch, ~, ~] =EnergyFun_convHull(Gatineau{1}.system, 0, 0, 4, 5);
                                  %Chelsea
[b_RF, ~, ~] =EnergyFun_convHull(Gatineau{1}.system, 0, 0, 5, 5);
                                  %R-farmers

if J==1
    structure_B( 1, 1 ).b_All_nodes(1,:)=b_Ca;
end

if J==2
    structure_B( 1, 1 ).b_All_nodes(1,:)=b_Ca;
    structure_B( 2, 1 ).b_All_nodes(1,:)=b_Ba;
end
if J==3
    structure_B( 1, 1 ).b_All_nodes(1,:)=b_Ca;
    structure_B( 2, 1 ).b_All_nodes(1,:)=b_Ba;
    structure_B( 3, 1 ).b_All_nodes(1,:)=b_Pa;
end
if J==4
    structure_B( 1, 1 ).b_All_nodes(1,:)=b_Ca;
```

```
    structure_B( 2, 1 ).b_All_nodes(1,:)=b_Ba;
    structure_B( 3, 1 ).b_All_nodes(1,:)=b_Pa;
    structure_B( 4, 1 ).b_All_nodes(1,:)=b_Ch;
end
if J==5
    structure_B( 1, 1 ).b_All_nodes(1,:)=b_Ca;
    structure_B( 2, 1 ).b_All_nodes(1,:)=b_Ba;
    structure_B( 3, 1 ).b_All_nodes(1,:)=b_Pa;
    structure_B( 4, 1 ).b_All_nodes(1,:)=b_Ch;
    structure_B( 5, 1 ).b_All_nodes(1,:)=b_RF;
end
%% Extracting data from SDDP (for myopic management you dont need these part)
% These lines uses Weekly_2_Daily function and convert the SDDP derived weekly beta,
% gamma, phi to daily for ST model
Daily_Beta = (Weekly_2_Daily(Gatineau,6,number_of_Years+1,Ens_hr)); % daily beta is the same for all nodes
ST_Output{1, 1}.cuts.Daily_Beta = Daily_Beta(:,1:operation_horizon++ Ens_hr); % placing daily beta in a structure
for j=11+1:11+J % daily gamma
Daily_Gamma= Weekly_2_Daily(Gatineau,j,number_of_Years+1,Ens_hr);
ST_Output{1, 1}.cuts.Daily_Gamma(j-11,1).Gamma = Daily_Gamma(:,1:operation_horizon + Ens_hr); % placing daily gamma in a structure
end
clear j
for j=6+1:6+J %daily phi
Daily_Phi= Weekly_2_Daily(Gatineau,j,number_of_Years+1,Ens_hr);
ST_Output{1, 1}.cuts.Daily_Phi(j-6,1).Phi = Daily_Phi(:,1:operation_horizon + Ens_hr+1); %placing daily phi in a structure
end
clear Daily_Gamma Daily_Phi j

%%%%%%%%%%%%%%%%%%%%%%%%%%%%%%%%%%%%%%%%%%%%%%%%%%%%%%%%%%%%%%%%%%%%%%%%%%%%%%%%%%%

nmb_of_Cuts=size(Gatineau{1, 1}.cuts{1, 1},1);  %number of
```

```
    backward opennings for cuts SDDP

%
    %%%%%%%%%%%%%%%%%%%%%%%%%%%%%%%%%%%%%%%%%%%%%%%%%%%%%%%%%%%%%%%%%%%%%%%%%%%%%%%

                    %MYOPIC MANAGEMENT scenario
% Daily_Beta =zeros(nmb_of_Cuts,operation_horizon+ Ens_hr);
% Daily_Gamma= zeros(nmb_of_Cuts,operation_horizon+ Ens_hr);
% Daily_Phi= zeros(nmb_of_Cuts,operation_horizon+ Ens_hr);
%
% ST_Output{1, 1}.cuts.Daily_Beta = Daily_Beta;
% for j= 1:J
% ST_Output{1, 1}.cuts.Daily_Gamma(j,1).Gamma = Daily_Gamma;
% ST_Output{1, 1}.cuts.Daily_Phi(j,1).Phi = Daily_Phi;
% end
%
    %%%%%%%%%%%%%%%%%%%%%%%%%%%%%%%%%%%%%%%%%%%%%%%%%%%%%%%%%%%%%%%%%%%%%%%%%%%%%%%


%% VARIALBLE DEFINITION:
% characteristics of the reservoirs (hydropowers):
S_In=Gatineau{1, 1}.sim1.st(2+31*52,:)'; %initial storage from SDDP
Smax=Gatineau{1, 1}.system.smax(1:J,1);
Smin=Gatineau{1, 1}.system.smin(1:J,1);
Rmax=Gatineau{1, 1}.system.rmax(1:J,1)/7;
Rmin=Gatineau{1, 1}.system.rmin(1:J,1)/7;
Ptmax=Gatineau{1, 1}.system.hp(1:J,1);
P1max=Gatineau{1, 1}.system.firmp(1:J,1);

%% Aineq2 : ST matrix for convexhull inequality
Sinq2=[];
for t=1:Ens_hr
        for p=1:J
            if p<4
                b=structure_B( p, 1 ).b_All_nodes(1,:);
                size_b=size(b,2);
                dumi_Sinq2=zeros(size_b,Ens_hr*J);
                clear sai1
                for b1=1:size_b
```

```
114                     sai1(b1,1)=b{1,b1}(3);
115                 end
116                 if t==1
117                     dumi_Sinq2(:,p)=-sai1/2;
118                     Sinq2=[Sinq2;dumi_Sinq2];
119                 else
120                     dumi_Sinq2(:,(t-2)*J+p)=-sai1/2;
121                     dumi_Sinq2(:,(t-1)*J+p)=-sai1/2;
122                     Sinq2=[Sinq2;dumi_Sinq2];
123                 end
124             end
125         end
126         if J==4
127             b=structure_B( J, 1 ).b_All_nodes(1,:);
128             dumi_Sinq2=zeros(1,Ens_hr*J);
129             sai2=b(3);
130             if t==1
131                 dumi_Sinq2(1,J)=-sai2/2;
132                 Sinq2=[Sinq2;dumi_Sinq2];
133             else
134                 dumi_Sinq2(1,t*J-J)=-sai2/2;
135                 dumi_Sinq2(1,t*J)=-sai2/2;
136                 Sinq2=[Sinq2;dumi_Sinq2];
137             end
138         end
139         if J==5
140             b=structure_B( J-1, 1 ).b_All_nodes(1,:);
141             dumi_Sinq2=zeros(1,Ens_hr*J);
142             sai2=b(3);
143             if t==1
144                 dumi_Sinq2(1,J-1)=-sai2/2;
145                 Sinq2=[Sinq2;dumi_Sinq2];
146             else
147                 dumi_Sinq2(1,t*J-1-J)=-sai2/2;
148                 dumi_Sinq2(1,t*J-1)=-sai2/2;
149                 Sinq2=[Sinq2;dumi_Sinq2];
150             end
151
152             b=structure_B( J, 1 ).b_All_nodes(1,:);
```

```
153             dumi_Sinq2=zeros(1,Ens_hr*J);
154             sai2=b(3);
155             if t==1
156                 dumi_Sinq2(1,J)=-sai2/2;
157                 Sinq2=[Sinq2;dumi_Sinq2];
158             else
159                 dumi_Sinq2(1,t*J-J)=-sai2/2;
160                 dumi_Sinq2(1,t*J)=-sai2/2;
161                 Sinq2=[Sinq2;dumi_Sinq2];
162             end
163
164         end
165 end
166  clear dumi_Sinq2
167
168 Rinq2=[];
169 for t=1:Ens_hr
170         for p=1:J
171             if p<4
172                 b=structure_B(p,1).b_All_nodes(1,:);
173                 size_b=size(b,2);
174                 dumi_Rinq2=zeros(size_b,Ens_hr*J);
175                 clear omega1
176                 for b1=1:size_b
177                     omega1(b1,1)=b{1,b1}(2);
178                 end
179                 dumi_Rinq2(:,(t-1)*J+p)=-omega1;
180                 Rinq2=[Rinq2;dumi_Rinq2];
181             end
182         end
183         if J==4
184             b=structure_B(J,1).b_All_nodes(1,:);
185             dumi_Rinq2=zeros(1,Ens_hr*J);
186             omega2=b(2);
187             dumi_Rinq2(:,t*J)=-omega2;
188             Rinq2=[Rinq2;dumi_Rinq2];
189         end
190         if J==5
191             b=structure_B(J-1,1).b_All_nodes(1,:);
```

```
192             dumi_Rinq2=zeros(1,Ens_hr*J);
193             omega2=b(2);
194             dumi_Rinq2(:,t*(J-1)+(t-1))=-omega2;
195             Rinq2=[Rinq2;dumi_Rinq2];
196
197             b=structure_B( J, 1 ).b_All_nodes(1,:);
198             dumi_Rinq2=zeros(1,Ens_hr*J);
199             omega2=b(2);
200             dumi_Rinq2(:,t*J)=-omega2;
201             Rinq2=[Rinq2;dumi_Rinq2];
202         end
203 end
204 clear dumi_Rinq2
205 Linq2=Rinq2*0;      %Linqu2
206
207 Ptinq2=[];
208 for t=1:Ens_hr
209         for p=1:J
210             if p<4
211                 b=structure_B( p, 1 ).b_All_nodes(1,:);
212                 size_b=size(b,2);
213                 dumi_Ptinq2=zeros(size_b,Ens_hr*J);
214                 dumi_Ptinq2(:,(t-1)*J+p)=ones(size_b,1);
215                 Ptinq2=[Ptinq2;dumi_Ptinq2];
216             end
217         end
218         if J==4
219             b=structure_B( J, 1 ).b_All_nodes(1,:);
220             dumi_Ptinq2=zeros(1,Ens_hr*J);
221             dumi_Ptinq2(:,t*J)=1;
222             Ptinq2=[Ptinq2;dumi_Ptinq2];
223         end
224         if J==5
225             b=structure_B( J-1, 1 ).b_All_nodes(1,:);
226             dumi_Ptinq2=zeros(1,Ens_hr*J);
227             dumi_Ptinq2(:,t*(J-1)+(t-1))=1;
228             Ptinq2=[Ptinq2;dumi_Ptinq2];
229
230             b=structure_B( J, 1 ).b_All_nodes(1,:);
```

```
231                 dumi_Ptinq2=zeros(1,Ens_hr*J);
232                 dumi_Ptinq2(:,t*J)=1;
233                 Ptinq2=[Ptinq2;dumi_Ptinq2];
234             end
235 end
236 clear dumi_Ptinq2
237 P1inq2=Rinq2*0;
238 P2inq2=Rinq2*0;
239 Finq2=P2inq2(:,1);
240
241 Ainq2=[Sinq2 Rinq2 Linq2 Ptinq2 P1inq2 P2inq2 Finq2];
242
243 %% Aeq : ST matrix for mass balance equation and energy equation:
244 [Aeq, ub, lb]= Matrix_Definition_Aeq(Ens_hr, Smax, Smin, Rmax, Rmin
        , Ptmax, J, P1max);
245
246 %% calling and Storing daily energy prices from SDDP:
247 ST_Output{1, 1}.system.pi = weekly_2_Daily_Power_Price(Gatineau{1,
        1}.system.pi, J, number_of_Years );      %Secondary p ($/MW/hr)
248 ST_Output{1, 1}.system.pi2 = weekly_2_Daily_Power_Price(Gatineau{1,
         1}.system.pi2, J, number_of_Years );        %total p ($/MW/hr)
249
250
251 %% ========================================================
252 for h= 1:number_of_hydro_models % this loop is for repeating 20
        times for the number of hydrological models
253 % for h= 1:1 %PERFECT FORECAST (this loop is for the perfect
        forecast
254 % scenario)
255 Repeater2=strcat('This is hydro-model loop ', num2str(h),' /20')
256 for l=start_Day:end_Day % This loop is for one time ST optimization
         (50 members, OH =2192 days)
257
258
259     %% Aineq : inequalities of FBF  and convexhull
260     %Aineq1 : Building the future-benefit-function inequality
            matrix for ST:
261     Sineq1=zeros((nmb_of_Cuts),(Ens_hr)*J);        %storage
262     for q=1:nmb_of_Cuts
```

```
263         for j=1:J
264             phi_nodes(1,j)=-ST_Output{1, 1}.cuts.Daily_Phi(j).Phi(q,
                    Ens_hr+l);
265         end
266       Sineq1((q-1)+1:q,J*(Ens_hr-1)+1:J*Ens_hr)= phi_nodes;
267       end
268
269       Rineq1=zeros((nmb_of_Cuts),(Ens_hr)*J);
                                        %release
270       Lineq1=zeros((nmb_of_Cuts),(Ens_hr)*J);
                                        %spill
271       Fineq1=ones((nmb_of_Cuts),1);
                                                %benefit to fo function
272       Ptin1=zeros((nmb_of_Cuts),(Ens_hr)*J);
                                        %total power
273       P1in1=zeros((nmb_of_Cuts),(Ens_hr)*J);
                                        %firm power
274       P2in1=zeros((nmb_of_Cuts),(Ens_hr)*J);
                                        %secondary power
275       Aineq1=[Sineq1 Rineq1 Lineq1 Ptin1 P1in1 P2in1 Fineq1];
                    %''the first A matrix''
276
277       Aineq=[Aineq1;Ainq2];     % Aineg
278
279 %%    Taking the initial storage for each loop
280 % Note taht the initial storage is the same for 50 members per day
281         if l==1
282             SS=S_In;
283         else
284             SS=storage1;
285         end
286 %% This loop repeats the optimization for each member for one day
287      for m=1:members
288 %% bineq
289 %bineq1 : The right side of benefir-to-go function
290 %binq2: The right side of convex-hull inequality
291 dumi_daily_Beta = ST_Output{1, 1}.cuts.Daily_Beta(:,Ens_hr+l-1);
292 bineq1=[];
293 for q=1:nmb_of_Cuts
```

```
294 %=========================
295       for j = 1:J
296           Gamma_node(j,1)=ST_Output{1, 1}.cuts.Daily_Gamma(j).Gamma(q
                ,Ens_hr+l-1);
297 %
    ==========================================================================


298           sum_Q_last_7_days(j,1)= sum(new_Inflow.new_Inflow(h).
                new_Inflow.ESF(l, j).ESF(Ens_hr-7+1:Ens_hr,m)); %lag1
299 %           sum_Q_last_7_days(j,1)= (sum(new_Inflow.new_Inflow(1).
    new_Inflow.Obs(j).Obs(l,:))) '; %Perfect forecast
300 %
    ==========================================================================


301           Gamma_Q(j,1)=Gamma_node(j,1)*sum_Q_last_7_days(j,1);
302       end
303 %=========================
304       dumi_bineq1=sum(Gamma_Q(1:J))+dumi_daily_Beta(q,1);
305       bineq1=[bineq1;dumi_bineq1];
306 end
307
308 binq2=binq2_function(l, Ens_hr, J, structure_B, SS);
309
310 bineq=[bineq1;binq2];
311
312 %% beq
313 %beq1 : The right side of mass balance equation
314 %beq2 : The right side of energy balance equation
315  beq1_dumi = [];
316  for j=1:J
317 %
    ==========================================================================


318  Inflow_m_d = (new_Inflow.new_Inflow(h).new_Inflow.ESF(l, j).ESF(:,
       m))';
319 %  Inflow_m_d = new_Inflow.new_Inflow(1).new_Inflow.Obs(j).Obs(l,:)
    ; %Perfect forecast
320 %
    ==========================================================================
```

```
321  Inflow_m_d (1,1)=SS(j,1)+ Inflow_m_d(1,1);
322  beq1_dumi = [beq1_dumi; Inflow_m_d];
323  end
324  beq1=[];
325  for q=1:Ens_hr
326   beq1_dumi2 = beq1_dumi(:,q);
327   beq1=[beq1;beq1_dumi2];
328  end
329 clear q j
330
331 beq2= zeros(J*Ens_hr,1);
332
333 beq=[beq1; beq2];     %beq
334
335 %% objective function:
336     Pi_Ens=[];
337     pi2_Ens=[];
338      for a=1:Ens_hr
339          Daily_Price_Pi_dumi= ST_Output{1, 1}.system.pi(l+a-1,1:J);
340          Daily_Price_Pi2_dumi= ST_Output{1, 1}.system.pi2(l+a-1,1:J)
                 ;
341
342          Pi_Ens=[Pi_Ens Daily_Price_Pi_dumi];  % $/MW/hr
343          pi2_Ens=[pi2_Ens Daily_Price_Pi2_dumi];          % $/MW/hr
344      end
345
346 Objective_f=[zeros(1,J*Ens_hr) zeros(1,J*Ens_hr) 0*ones(1,J*Ens_hr)
       zeros(1,J*Ens_hr) Pi_Ens.*24  pi2_Ens.*24 1];
347 % Objective_f=[zeros(1,J*Ens_hr) zeros(1,J*Ens_hr) 0*ones(1,J*
     Ens_hr) zeros(1,J*Ens_hr) Pi_Ens.*24  pi2_Ens.*24 0]; %MYOPIC
     MANAGEMENT
348
349 %% ST optimization
350 [ESF_Opt, duals, fval] = ...
351      A_maximise(Objective_f, Aeq, beq, Aineq, bineq, lb, ub, 1);
352
353 %% OUTPUTS
354 %output for each member:
```

```
355         release(:,m)=ESF_Opt(71:75);
356         storage2(:,m)=ESF_Opt(1:5);
357         spill2(:,m)=ESF_Opt(141:145);
358         pt(:,m)= ESF_Opt(211:215);
359
360
361
362 OBF = Objective_f(end)*ESF_Opt(end);
363 ESF.OBF(l,:) = OBF ;
364 IBOBF = Objective_f(1:end-1)*ESF_Opt(1:end-1);
365 ESF.IBOBF(l,:) = IBOBF ;
366
367 % For Perfect forecast remove this for:
368 for j= 1:5
369             ESF.Inflow_Mean(1,j).Mean(l,:)= mean(new_Inflow.new_Inflow
                    (h).new_Inflow.ESF(l, j).ESF ,2);
370             ESF.Inflow_First_Day(1,j).First_Day(l,m)= new_Inflow.
                    new_Inflow(h).new_Inflow.ESF(l, j).ESF(1,m);
371 end
372       end  %for m
373
374 % average of  50 members:
375  release_mean_m = mean(release,2);
376  storage2_mean_m = mean(storage2,2);
377  spill_mean_m = mean(spill2,2);
378  pt_mean_m = mean(pt,2);
379
380  %For Perfect forecast remove this for:
381 for j=1:J
382 Q_member_mean = mean(new_Inflow.new_Inflow(h).new_Inflow.ESF(l, j).
      ESF,2);
383 ESF.Q_member_mean (l,j) = Q_member_mean(j);
384 end
385
386 % storing the average of  50 members in the structure:
387     for j=1:5
388  Q(j) = new_Inflow.new_Inflow(h).new_Inflow.Obs(j).Obs(l);
389  ESF.s(l,j)= storage2_mean_m (j);
390  ESF.r(l,j)= release_mean_m (j);
```

```
391   ESF.l(l,j)= spill_mean_m (j);
392   ESF.pt(l,j)= pt_mean_m(j);
393      end
394
395
396 %    % FOR PERFECT FORECAST ACTIVATE THIS FOR:
397 %        for j=1:5
398 %   Q(j) = new_Inflow.new_Inflow(2).new_Inflow.Obs(j).Obs(l);
399 %   ESF.s(l,j)= storage2 (j);
400 %   ESF.r(l,j)= release (j);
401 %   ESF.l(l,j)= spill2 (j);
402 %   ESF.pt(l,j)= pt(j);
403 %      end
404
405 %    % FOR PERFECT FORECAST:
406 % storage1 = storage2;
407
408 %% SIMULATION
409    % FOR PERFECT FORECAST remove the simulation:
410
411 % for node 1:
412 storage1_1 = Q(1) + SS(1) - release_mean_m (1)- spill_mean_m(1) ;
413      if storage1_1 < Smin(1)
414          storage1_1 = Smin(1);
415      else
416          if storage1_1 > Smax(1)
417              spill1_1 = storage1_1 - Smax(1);
418              storage1_1 = Smax(1);
419          else
420              spill1_1 = 0;
421          end
422      end
423
424 % for node 2:
425 storage1_2 = Q(2) + SS(2) - release_mean_m (2) - spill_mean_m(2) +
      ...
426      release_mean_m (1) + spill1_1 + spill_mean_m(1);
427
428      if storage1_2 < Smin(2)
```

```
429         storage1_2 = Smin(2);
430     else
431         if storage1_2 > Smax(2)
432             spill1_2 = storage1_2 - Smax(2);
433             storage1_2 = Smax(2);
434         else
435             spill1_2 = 0;
436         end
437     end
438 % for node 3:
439 storage1_3 = Q(3) + SS(3) - release_mean_m (3) - spill_mean_m(3) +
    ...
440     release_mean_m (2) + spill1_2 + spill_mean_m(2);
441
442     if storage1_3 < Smin(3)
443         storage1_3 = Smin(3);
444     else
445         if storage1_3 > Smax(3)
446             spill1_3 = storage1_3 - Smax(3);
447             storage1_3 = Smax(3);
448         else
449             spill1_3 = 0;
450         end
451     end
452 % for node 4:
453 storage1_4 = Q(4) + SS(4) - release_mean_m (4) - spill_mean_m(4) +
    ...
454     release_mean_m (3) + spill1_3 + spill_mean_m(3);
455
456         if storage1_4 > Smax(4)
457             spill1_4 = storage1_4 - Smax(4);
458             storage1_4 = Smax(4);
459         else
460             spill1_4 = 0;
461         end
462
463 % for node 5:
464 storage1_5 = Q(5) + SS(5) - release_mean_m (5) - spill_mean_m(5) +
    ...
```

```
465      release_mean_m (4) + spill1_4 + spill_mean_m(4);
466
467          if storage1_5 > Smax(5)
468              spill1_5 = storage1_5 - Smax(5);
469              storage1_5 = Smax(5);
470          else
471              spill1_5 = 0;
472          end
473
474
475 storage1 = [storage1_1; storage1_2; storage1_3; storage1_4;
        storage1_5];
476
477 % storing the simulated spills
478 for j= 1:5
479      ESF.st(l,j)= storage1(j);
480 end
481     ESF.l_sim(l,1) = spill1_1;
482     ESF.l_sim(l,2) = spill1_2;
483     ESF.l_sim(l,3) = spill1_3;
484     ESF.l_sim(l,4) = spill1_4;
485     ESF.l_sim(l,5) = spill1_5;
486
487 end %for l
488
489 ESF_All.ESF(h).ESF = ESF;  %%FOR PERFECT FORECAST deactivate this
        line
490 end %for h
491
492 toc;
```

Bibliographie

Ahmad, A., El-shafie, A., 2014. Reservoir Optimization in Water Resources : a Review. Water Resources Management , 3391–3405doi :10.1007/s11269-014-0700-5.

Alemu, E.T., Palmer, R.N., Polebitski, A., Meaker, B., 2011. Decision Support System for Optimizing Reservoir Operations Using Ensemble Streamflow Predictions. Journal of water Resources Planning and Management 137, 72–82. doi :10.1061/(ASCE)WR.1943-5452.0000088.

Archibald, T.W., Buchanan, C.S., Mckinnon, K.I.M., Thomas, L.C., 1999. Nested Benders decomposition and dynamic programming for reservoir optimisation. Journal of the Operational Research Society , 468–479.

Arena, C., Cannarozzo, M., Mazzola, M.R., 2017. Exploring the Potential and the Boundaries of the Rolling Horizon Technique for the Management of Reservoir Systems with over-Year Behaviour. Water Resources Management 31, 867–884. doi :10.1007/s11269-016-1550-0.

Bellman, R.E., 1957. Dynamic programming. Princeton University Press, Princeton, N.J.

Boucher, M.A., Tremblay, D., Delorme, L., Perreault, L., Anctil, F., 2012. Hydro-economic assessment of hydrological forecasting systems. Journal of Hydrology 416-417, 133–144. URL : http://dx.doi.org/10.1016/j.jhydrol.2011.11.042, doi :10.1016/j.jhydrol.2011.11.042.

Bourdin, D.R., Fleming, S.W., Stull, R.B., 2012. Streamflow Modelling : A Primer on Applications, Approaches and Challenges. Atmosphere-Ocean 50, 507–536. doi :10.1080/07055900.2012.734276.

Cerisola, S., Latorre, J.M., Ramos, A., 2012. Stochastic dual dynamic programming applied to nonconvex hydrothermal models. European Journal of Operational Research 218, 687–697. URL : http://dx.doi.org/10.1016/j.ejor.2011.11.040, doi :10.1016/j.ejor.2011.11.040.

Cloke, H.L., Pappenberger, F., 2009. Ensemble flood forecasting : A review. Journal of Hydrology 375, 613–626. URL : http://dx.doi.org/10.1016/j.jhydrol.2009.06.005, doi :10.1016/j.jhydrol.2009.06.005.

Fan, F.M., Schwanenberg, D., Alvarado, R., Assis dos Reis, A., Collischonn, W., Naumman, S., 2016. Performance of Deterministic and Probabilistic Hydrological Forecasts for the Short-Term Optimization of a Tropical Hydropower Reservoir. Water Resources Management 30, 3609–3625. URL : http://dx.doi.org/10.1007/s11269-016-1377-8, doi :10.1007/s11269-016-1377-8.

Ficchì, A., Raso, L., Dorchies, D., Pianosi, F., Malaterre, P., Overloop, P.V., 2015. Optimal Operation of the Multireservoir System in the Seine River Basin Using Deterministic and Ensemble Forecasts 7, 1–12. doi :10.1061/(ASCE)WR.1943-5452.0000571.

Fraley, C., Raftery, A.E., Gnetting, T., 2010. Calibrating Multimodel Forecast Ensembles with Exchangeable and Missing Members Using Bayesian Model Averaging. American Meteorological Society , 190–202doi :10.1175/2009MWR3046.1.

Georgakakos, A.P., 2006. DECISION SUPPORT SYSTEMS FOR WATER RESOURCES MANAGEMENT : NILE BASIN APPLICATIONS AND FURTHER NEEDS Aris P. Georgakakos .

Gjelsvik, A., Mo, B., Haugstad, A., 2010. Long- and Medium-term Operations Planning and StochasticModelling in Hydro-dominated Power Systems Based on Stochastic Dual Dynamic Programming. Handbook of Power Systems I URL : http://link.springer.com/10.1007/978-3-642-12686-4, doi :10.1007/978-3-642-12686-4.

Goor, Q., Kelman, R., Tilmant, A., 2011. Optimal Multipurpose-Multireservoir Operation Model with Variable Productivity of Hydropower Plants. Journal of Water Resources Planning and Management 137, 258–267. doi :10.1061/(ASCE)WR.1943-5452.

Goor, Q., Kelman, R., Tilmant, A., 2012. Exploring the Water-Thermoelectric Power Nexus. Journal of Water Resources Planning and Management 138, 491–501. doi :10.1061/(ASCE)WR.1943-5452.

Karamouz, M., Szidarovszky, F., Zahraie, B., 2003. Water Resources Systems Analysis with Emphasis on Conflict Resolution. LEWIS PUBLISHERS.

Kristiansen, T., 2004. Financial risk management in the electric power industry using stochastic optimization. Advanced Modeling and Optimization 6, 17–24. URL : http://camo.ici.ro/journal/vol6/v6b2.pdf.

Labadie, J.W., 2004. Optimal Operation of Multireservoir Systems : State-of-the-Art Review. Journal of Water Resources Planning and Management 130, 93–111. doi :10.1061/(ASCE)0733-9496(2004)130:2(93).

Lamontagne, J.R., Stedinger, J.R., 2014. Short-Term Hydropower Optimization Using A Time-Decomposition Algorithm. International Conference on Hydroinformatics .

Lee, Y., Kim, S.K., Ko, I.H., 2006. Two-Stage Stochastic Linear Programming Model for Coordinated Multi-Reservoir Operation. Operating Reservoirs in Changing Conditions ASCE , 205–214.

Macian-Sorribes, H., Tilmant, A., Pulido-Velazques, M., 2017. Water Resources Research. Water Resources Research 53, 1407–1423. doi :10.1002/2014WR015716.

Matheson, J.E., Winkler, R.L., 1976. Scoring Rules for Continuous Probability Distributions. Management science 22, 1087–1096.

Pereira, M., Pinto, L., 1991. Multi-stage stochastic optimization applied to energy planning. Mathematical Programming 52, 359–375. URL : http://link.springer.com/article/10.1007{%}2FBF01582895, doi :10.1007/BF01582895.

Pereira, M.V.F., 1989. Optimal stochastic operations scheduling of large hydroelectric systems. International Journal of Electrical Power and Energy Systems 11, 161–169. doi :10.1016/0142-0615(89)90025-2.

Pereira-Cardenal, S.J., Mo, B., Gjelsvik, A., Riegels, N.D., Arnbjerg-Nielsen, K., Bauer-Gottwein, P., 2016. Joint optimization of regional water-power systems. Advances in Water Resources 92, 200–207. doi :10.1016/j.advwatres.2016.04.004.

Perrin, C., 2000. Vers une amélioration d ' un modèle global pluie-débit To cite this version : HAL Id : tel-00006216. Ph.D. thesis. Institut National Polytechnique de Grenoble - INPG.

Pina, J., 2017. The value of hydrological information in mutireservoir systems operation. Ph.D. thesis. Laval University.

Pina, J., Tilmant, A., Côté, P., 2017a. Optimizing multireservoir system operating policies using exogenous hydrologic variables .

Pina, J., Tilmant, A., Ph, D., Anctil, F., Ph, D., 2017b. Horizontal Approach to Assess the Impact of Climate Change on Water Resources Systems. Journal of Water Resources Planning and Management 143, 1–11. doi :10.1061/(ASCE)WR.1943-5452.0000737.

Poorsepahy-Samian, H., Espanmanesh, V., Zahraie, B., 2016. Improved Inflow Modeling in Stochastic Dual Dynamic Programming. Journal of Water Resources Planning and Management 142, 04016065. URL : http://ascelibrary.org/doi/10.1061/{%}28ASCE{%}29WR.1943-5452.0000713, doi :10.1061/(ASCE)WR.1943-5452.0000713.

Rani, D., Moreira, M.M., 2010. Simulation-optimization modeling : A survey and potential application in reservoir systems operation. Water Resources Management 24, 1107–1138. doi :10.1007/s11269-009-9488-0.

Raso, L., Malaterre, P.o., Bader, J.c., 2017. Effective Streamflow Process Modeling for Optimal Reservoir Operation Using Stochastic Dual Dynamic Programming 143, 1–11. doi :10.1061/(ASCE)WR.1943-5452.0000746.

Séguin, S., Audet, C., Côté, P., 2017. Scenario-Tree Modeling for Stochastic Short-Term Hydropower Operations Planning 143, 1–12. doi :10.1061/(ASCE)WR.1943-5452.0000854.

Seif, A., Hipel, K.W., 2001. Interior-Point Method for Reservoir Operation with Stochastic Inflows. Journal of Water Resources Planning and Management 127, 48–57.

Seiller, G., Anctil, F., Perrin, C., 2012. Multimodel evaluation of twenty lumped hydrological models under contrasted climate conditions. Hydrology and Earth System Sciences 16, 1171–1189. doi :10.5194/hess-16-1171-2012.

Shapiro, A., Tekaya, W., Da Costa, J.P., Soares, M.P., 2013. Risk neutral and risk averse Stochastic Dual Dynamic Programming method. European Journal of Operational Research 224, 375–391. URL : http://dx.doi.org/10.1016/j.ejor.2012.08.022, doi :10.1016/j.ejor.2012.08.022.

Sreenivasan, K.R., Vedula, S., 1996. Reservoir operation for hydropower optimization : A chance-constrained approach. Sadhana 21, 503–510. doi :10.1007/BF02745572.

Tejada-Guibert, J.A., Johnson, S.A., Stedinger, J.R., 1993. Comparison of two approaches for implementing multireservoir operating policies derived using stochastic dynamic programming. Water Resources Research 29, 3969–3980. doi :10.1029/93WR02277.

Tilmant, A., Kelman, R., 2007. A stochastic approach to analyze trade-offs and risks associated with large-scale water resources systems. Water Resources Research 43. doi :10.1029/2006WR005094.

Tilmant, A., Kinzelbach, W., 2012. The cost of noncooperation in international river basins. Water Resources Research 48, 1–12. doi :10.1029/2011WR011034.

Tilmant, A., Pinte, D., Goor, Q., 2008. Assessing marginal water values in multipurpose multireservoir systems via stochastic programming. Water Resources Research 44, 1–17. doi :10.1029/2008WR007024.

Wang, L., Koike, T., Ikeda, M., Tinh, D.N., Nyunt, C.T., Saavedra, O., Nguyen, L.C., Sap, T.V., Tamagawa, K., Ohta, T., 2014. Optimizing Multidam Releases in Large River Basins by Combining Distributed Hydrological Inflow Predictions with Rolling-Horizon Decision Making. Journal of Water Resources Planning and Management 140, 05014006. URL : http://ascelibrary.org/doi/10.1061/{%}28ASCE{%}29WR.1943-5452.0000452, doi :10.1061/(ASCE)WR.1943-5452.0000452.

Yao, H., Georgakakos, A., 2001. Assessment of folsom lake response to historical and potential future climate scenarios 2. Reservoir management. Journal of Hydrology 249, 176–196. doi :10.1016/S0022-1694(01)00418-8.

Yeh, W.W., Becker, L., 1982. Multiobjective analysis of multireservoir operations. Water Resources Research 18, 1326–1336. doi :10.1029/WR018i005p01326.

You, J.Y., Cai, X., 2008. Determining forecast and decision horizons for reservoir operations under hedging policies. Water Resources Research 44, 1–14. doi :10.1029/2008WR006978.

Zahraie, B., Karamouz, M., 2004. Hydropower Reservoirs Operation : A Time Decomposition Approach. Scientia Iranica 11, 92–103.

Zhao, T., Cai, X., Yang, D., 2011. Effect of streamflow forecast uncertainty on real-time reservoir operation. Advances in Water Resources 34, 495–504. URL : http://dx.doi.org/10.1016/j.advwatres.2011.01.004, doi :10.1016/j.advwatres.2011.01.004.

Zhao, T., Yang, D., Cai, X., Zhao, J., Wang, H., 2012. Identifying effective forecast horizon for real-time reservoir operation under a limited inflow forecast. Water Resources Research 48, 1–15. doi :10.1029/2011WR010623.

Zhao, T., Zhao, J., 2014. Joint and respective effects of long- and short-term forecast uncertainties on reservoir operations. Journal of Hydrology 517, 83–94. URL : http://dx.doi.org/10.1016/j.jhydrol.2014.04.063, doi :10.1016/j.jhydrol.2014.04.063.

Zhao, T., Zhao, J., Yang, D., 2014. Improved Dynamic Programming for Hydropower Reservoir Operation. Journal of Water Resources Planning and Management 140, 365–374. doi :10.1061/(ASCE)WR.1943-5452.0000343.